the FEBS Journal

# Variation in pantothenate kinase type determines the pantothenamide mode of action and impacts on coenzyme A salvage biosynthesis

Marianne de Villiers*, Leanne Barnard*, Lizbé Koekemoer, Jacky L. Snoep and Erick Strauss

Department of Biochemistry, Stellenbosch University, South Africa

**Keywords**
coenzyme A; growth inhibition; pantetheine; pantothenamide; pantothenate kinase

**Correspondence**
E. Strauss, Department of Biochemistry, Stellenbosch University, Stellenbosch 7600, South Africa
Fax: +27 21 808 5863
Tel: +27 21 808 5866
E-mail: estrauss@sun.ac.za

*These authors contributed equally to this work.

(Received 30 May 2014, revised 18 July 2014, accepted 18 August 2014)

doi:10.1111/febs.13013

*N*-substituted pantothenamides are analogues of pantothenic acid, the vitamin precursor of CoA, and constitute a class of well-studied bacterial growth inhibitors that show potential as new antibacterial agents. Previous studies have highlighted the importance of pantothenate kinase (PanK; EC 2.7.1.33) (the first enzyme of CoA biosynthesis) in mediating pantothenamide-induced growth inhibition by one of two proposed mechanisms: first, by acting on the pantothenamides as alternate substrates (allowing their conversion into CoA antimetabolites, with subsequent effects on CoA- and acyl carrier protein-dependent processes) or, second, by being directly inhibited by them (causing a reduction in CoA biosynthesis). In the present study we used structurally modified pantothenamides to probe whether PanKs interact with these compounds in the same manner. We show that the three distinct types of eubacterial PanKs that are known to exist ($PanK_I$, $PanK_{II}$ and $PanK_{III}$) respond very differently and, consequently, are responsible for determining the pantothenamide mode of action in each case: although the promiscuous $PanK_I$ enzymes accept them as substrates, the highly selective $PanK_{III}$s are resistant to their inhibitory effects. Most unexpectedly, *Staphylococcus aureus* PanK (the only known example of a bacterial $PanK_{II}$) experiences uncompetitive inhibition in a manner that is described for the first time. In addition, we show that pantetheine, a CoA degradation product that closely resembles the pantothenamides, causes the same effect. This suggests that, in *S. aureus*, pantothenamides may act by usurping a previously unknown role of pantetheine in the regulation of CoA biosynthesis, and validates its PanK as a target for the development of new antistaphylococcal agents.

## Introduction

The *N*-substituted pantothenamides are a class of pantothenic acid (Pan, vitamin $B_5$) analogues that were first described in 1970 as growth inhibitors of selected lactic acid bacteria and *Escherichia coli* [1]. Because Pan is the biosynthetic precursor of the universal acyl group carrier CoA (Fig. 1A), which serves to activate

**Abbreviations**
ACP, acyl carrier protein; AcpH, [ACP]hydrolase; dN5, DL-4′-deoxy-*N*-pentylpantothenamide; DPCK, dephospho-CoA kinase; *Ec*$PanK_I$, *Escherichia coli* type I pantothenate kinase; HoPanAm, homopantothenamide; HoPan, homopantothenic acid; HRMS, high resolution mass spectrometry; LDH, lactate dehydrogenase; MIC, minimal inhibitory concentration; N354-Pan, *N*-[2-(1,3-benzodioxol-5-yl)ethyl] pantothenamide; N5-Pan, *N*-pentyl pantothenamide; N7-Pan, *N*-heptyl pantothenamide; *n*-PanAm, *n*-pantothenamide; PanK, pantothenate kinase; Pan, pantothenic acid; PantSH, pantetheine; PK, pyruvate kinase; P-Pan, 4′-phosphopantothenic acid; P-PantSH, 4′-phosphopantetheine; PPAT, phosphopantetheine adenylyltransferase; *Sa*$PanK_{II}$, *Staphylococcus aureus* type II pantothenate kinase; α-PanAm, α-pantothenamide.

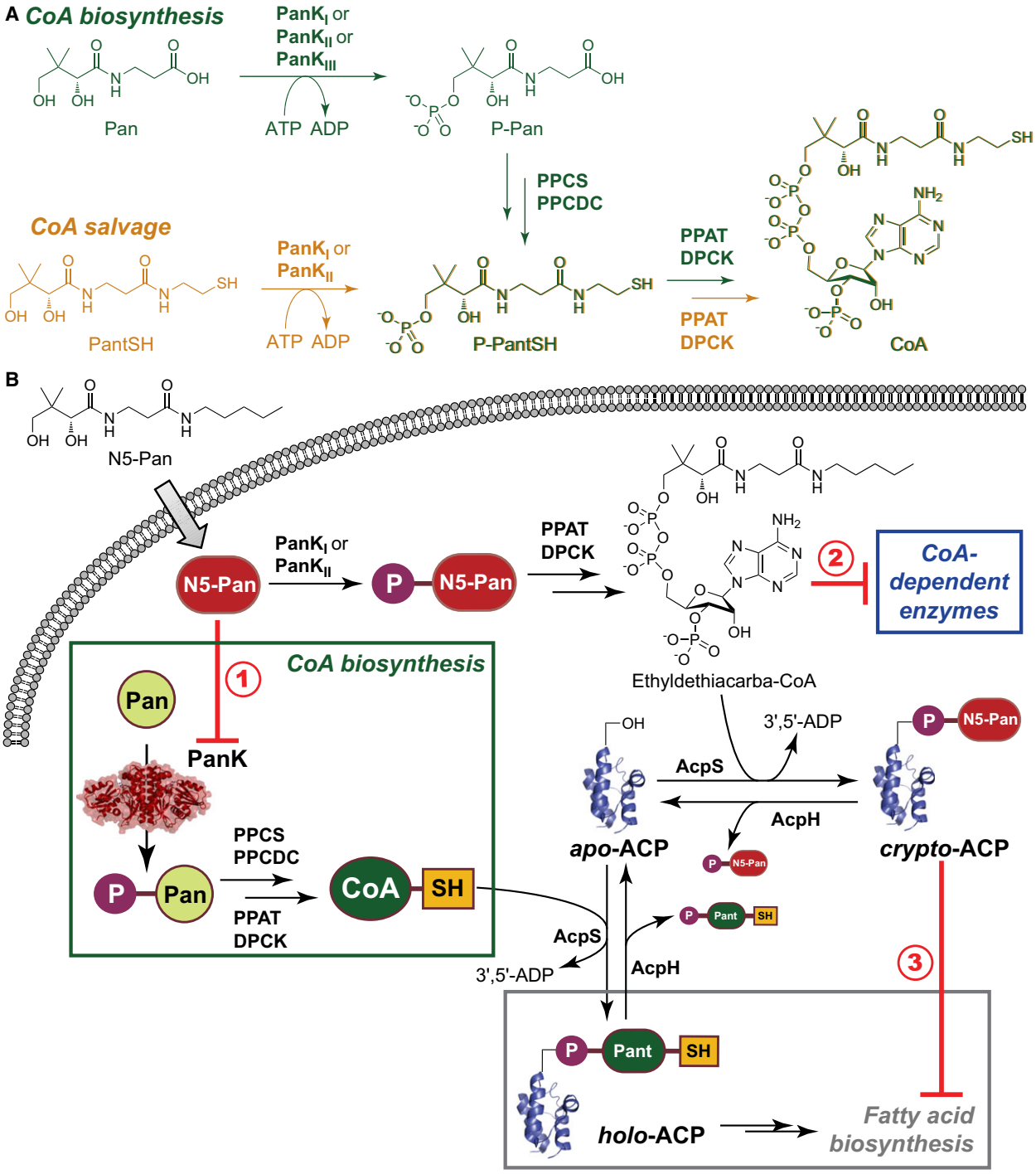


**Fig. 1.** Biosynthesis of CoA and the potential targets of the pantothenamide mode of action. (A) Biosynthesis of CoA from Pan in the five-step pathway catalyzed by panothenate kinase (PanK), phosphopantothenoylcysteine synthetase (PPCS), phosphopantothenoylcysteine decarboxylase (PPCDC), phosphopantetheine adenylyltransferase (PPAT) and dephospho-CoA kinase (DPCK), or from PantSH in the three-step salvage pathway consisting of PanK, PPAT and DPCK. (B) The three major biological targets of N5-Pan: (i) PanK, the first CoA biosynthetic enzyme; (ii) CoA-dependent enzymes, after its transformation into the antimetabolite ethyldethiacarba-CoA; and (iii) fatty acid biosynthesis, when ethyldethiacarba-CoA serves as substrate for AcpS to form a *crypto*-ACP instead of the catalytically active *holo*-ACP. *Holo*- and *crypto*-ACP are recycled back to *apo*-ACP by AcpH.

these groups for both acyl transfer reactions and biological Claisen condensation reactions [2], pantothenamides have raised much interest as antimetabolite-based lead compounds for the development of new selective antimicrobial agents [3]. Although recent studies have again highlighted the potential of these compounds [4–6], attempts at improving their potency are hampered by the fact that their mode of action still has not been unambiguously defined and appears to show variation between different organisms.

The first mode of action study, which was conducted in *E. coli* using *N*-pentyl pantothenamide (N5-Pan), the prototypical example of the class, showed that it is transformed into the CoA antimetabolite ethyldethiacarba-CoA by three of the five CoA biosynthetic enzymes (Fig. 1B) [7]. These enzymes are pantothenate kinase (PanK; EC 2.7.1.33), the first enzyme of the pathway that usually catalyzes the ATP-dependent phosphorylation of Pan to give 4′-phosphopantothenic acid (P-Pan), and the fourth and fifth enzymes phosphopantetheine adenylyltransferase (PPAT) and dephospho-CoA kinase (DPCK), which transform 4′-phosphopantetheine (P-PantSH) into CoA through the addition of adenylyl and phosphate groups, respectively (Fig. 1A). Moreover, the formation of ethyldethiacarba-CoA took place faster than the five-step conversion of Pan into CoA when conducted under competitive conditions *in vitro*. This suggested that N5-Pan exerted its inhibitory effect by reducing the rate of CoA synthesis, and/or through its biosynthetic product inhibiting enzymes and processes dependent on CoA.

A second study focused on fatty acid biosynthesis as the target for pantothenamide-induced bacterial growth inhibition, based on the essential requirement of the *holo*-acyl carrier protein (*holo*-ACP) in type II fatty acid synthase systems (as found in *E. coli*) [8]. Although *holo*-ACP is formed when [ACP]synthase transfers the P-PantSH group from CoA to *apo*-ACP [9], it is also possible for CoA analogues such as ethyldethiacarba-CoA to serve as the substrate instead; this leads to the formation of *crypto*-ACPs that do not have the requisite thiol group and are therefore unable to act as acyl carriers (Fig. 1B). N5-Pan treatment led to the formation of the N5-Pan-containing *crypto*-ACP (ethyldethiacarba-ACP) as predicted, and to a reduction in normal *holo*-ACP levels. CoA levels apparently remained unaffected. Ethyldethiacarba-ACP was also shown to accumulate and persist in N5-Pan-treated cells even after N5-Pan was removed from the culture, suggesting that ethyldethiacarba-ACP is a poor substrate for the [ACP]hydrolase (AcpH) that is responsible for ACP prosthetic group turnover [10,11]. In combination, these factors were considered to result in the complete inhibition of fatty acid biosynthesis; this has subsequently been hailed as the major target for pantothenamide-induced growth inhibition in bacteria.

Several subsequent studies have drawn this assertion into question. First, studies of the purified AcpH and *E. coli* strains in which the *acpH* gene was either knocked out or overexpressed indicated that the accumulation of ethyldethiacarba-ACP following N5-Pan treatment is not a result of reduced ACP turnover because this *crypto*-ACP was found to be readily hydrolyzed by AcpH [12]. Instead, N5-Pan treatment caused a significant reduction in the CoA pool (in contrast to the previous findings), indicating N5-Pan-mediated inhibition of CoA biosynthesis. Attempts at identifying the specific target by individual overexpression of the CoA biosynthetic genes failed because these strains instead showed an increase in N5-Pan sensitivity. This again pointed to the increased flux of the antimetabolite through the pathway as an important additional determinant of pantothenamide-meditated growth inhibition. Second, an investigation of pantothenamide-mediated inhibition of *Staphylococcus aureus* identified PanK as its point of action [13] because only pantothenamides that caused inhibition of the *S. aureus* PanK enzyme *in vitro* (using a standard kinase assay that couples ADP formation to NADH reduction) showed cell growth inhibition. However, a subsequent study revisited these results and used [$\gamma$-$^{32}$P]ATP to demonstrate that *S. aureus* PanK phosphorylates both N5-Pan and its heptyl analogue N7-Pan, and that this (as in the case of *E. coli*) also leads to the formation of modified *crypto*-ACPs and the inhibition of fatty acid synthesis [14]. However, because no studies have investigated the relative importance of the two inhibition modes, the role of PanK in the pantothenamide-mediated growth inhibition of *S. aureus* remains unresolved.

Although the exact mode of action of the pantothenamides still remains a matter of debate, these studies have all clearly highlighted the importance of PanK in mediating their growth inhibitory effects by one of two mechanisms: (a) by acting as the cellular target of inhibition, leading to the suppression of CoA biosynthesis or (b) by accepting pantothenamides as substrates, thereby allowing them to be converted into CoA analogues that exert their effects on CoA- and ACP-dependent processes. Unfortunately, structure–activity relationship studies that set out to establish a correlation between the growth inhibitory potency of a a pantothenamide and its potential to act as either an

inhibitor or substrate of the target organism's PanK have not been able to provide more insight into the enzyme's apparent dual role in pantothenamide-based inhibition [15,16].

Importantly, the distinction between a pantothenamide acting as either a PanK substrate or inhibitor may be linked to other aspects of CoA metabolism. For example, only organisms with PanKs that show poor substrate selectivity are able to form CoA from pantetheine (PantSH) (a CoA-derived degradation product structurally related to the pantothenamides) by means of a salvage pathway made up of PanK, PPAT and DPCK (Fig. 1A) [2]. PanKs occur as one of three distinct forms, known as type I, type II and type III PanK enzymes, respectively [17–20], with only $PanK_I$ and $PanK_{II}$ (the subscript denotes the type) showing activity towards both Pan and PantSH [21]. Organisms such as *Pseudomonas aeruginosa* that have $PanK_{III}$ enzymes cannot salvage CoA from pantetheine [22] and are also resistant to pantothenamide-induced growth inhibition [17,20]. This suggests that the inhibition mode of the pantothenamides (as structural mimics of PantSH) may be linked to the targeted organism's PanK type and its ability to salvage CoA.

In the present study, we explored the existence of such links through a combination of bacterial cell growth inhibition and kinetic characterization studies. We find that PanK type is the major determinant of the pantothenamide mode of action, and particularly so in *S. aureus*, which has a unique CoA metabolism supported by a $PanK_{II}$ with several exceptional features [14,20]. These results not only provide significant new insights for antimetabolite-based antimicrobial drug design, but also add to our understanding of the implications of PanK diversity for CoA metabolism and regulation.

## Results

### Pantothenamide library and study design

The link between PanK type and pantothenamide-induced bacterial cell growth inhibition was investigated using a library of *N*-substituted pantothenamides that was previously prepared in our laboratory and recently used to identify antiplasmodial pantothenamides that are resistant to pantetheinase-mediated degradation [5,23]. The library was constructed from Pan and two Pan analogues: α-pantothenic acid, which has the β-alanine of Pan replaced with glycine, and homopantothenic acid (HoPan) in which it is exchanged for γ-aminobutyric acid. The acids were subsequently coupled to 47 different amines representing a variety of chemical motifs, yielding three sets of pantothenamides, referred to as α-pantothenamides (α-PanAm), *n*-pantothenamides (*n*-PanAm, where *n* signifies 'normal') and homopantothenamides (HoPanAm), respectively (Table 1).

Although α-pantothenic acid has not previously been studied in the context of PanK and/or CoA inhibitors, HoPan was shown to act as a competitive inhibitor of a murine $PanK_{II}$ (*Mm*PanK1α) and to negatively affect CoA levels in mice *in vivo* [24]. The same result was found in insect cells [25]. By contrast, *E. coli* type I PanK (*Ec*$PanK_I$), which is known to accept a range of pantothenic acid analogues [21], does not accept HoPan as a substrate, nor is it significantly inhibited by it [15,24,26]. This diverse response indicated that such modifications in the Pan structure could successfully be used to probe PanK activity and inhibition.

### Organisms with different PanK types exhibit different pantothenamide-induced growth inhibition profiles

Three bacterial species, representing all three PanK types, were selected to evaluate the potency of the pantothenamide library members: *E. coli*, a Gram-negative bacterium with a typical $PanK_I$, the Gram-positive *S. aureus*, the only bacterium known to have an active (albeit atypical) $PanK_{II}$ (normally only eukaryotes have $PanK_{II}$ enzymes) and *P. aeruginosa*, a Gram-negative $PanK_{III}$-containing bacterium [2]. Although *P. aeruginosa* has been shown to be resistant to N5-Pan inhibition as a result of the selectivity of its $PanK_{III}$ enzyme [20], it was included in the present study because we considered that the smaller α-PanAm series could potentially be accommodated in its active site. As in several previous studies [16,27], growth inhibition assays were conducted in 1% tryptone (pancreatic digest of casein), a medium that contains low amounts (< 1 μM) of Pan [28]. Such Pan concentrations are not strictly physiologically relevant to humans with bacterial infections because the concentration of total Pan (i.e. free Pan and Pan bound up in CoA and other Pan-derived metabolites) in human whole blood ranges between 1 and 3 μM [29,30]. However, it allows susceptibility data to be obtained under conditions where Pan is not sufficiently abundant to counteract any potential inhibition, and therefore serves the point of investigating the mode of action of these compounds.

Susceptibility tests were performed by obtaining minimal inhibitory concentration (MIC) values for those compounds that showed inhibition in initial screens performed at 200 and 50 μM, respectively. The structures and MIC values for the pantothenamides

**Table 1.** MIC values for the inhibition of *E. coli* or *S. aureus* grown for 20 h in 1% tryptone medium in the presence of the indicated pantothenamides at different concentrations. The reported values represent the mean of two or more independent experiments; the errors indicate the range/2. References to compounds tested in previous studies are provided in the main text.

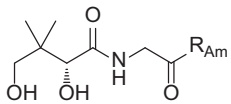

α-PanAm

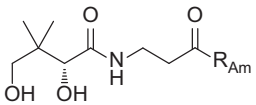

*n*-PanAm

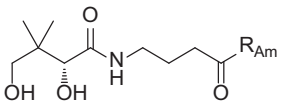

HoPanAm

| PanAm entry | $R_{Am}$ group | *E. coli* MIC (μM) | | | *S. aureus* MIC (μM) | | |
|---|---|---|---|---|---|---|---|
| | | α-PanAm | *n*-PanAm | HoPanAm | α-PanAm | *n*-PanAm | HoPanAm |
| 1 |  | **50–200** | > 200 | > 200 | > 200 | **30.8 ± 4.3** | > 200 |
| 2 | 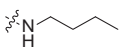 | **50–200** | > 200 | > 200 | > 200 | **50–200** | > 200 |
| 3 | 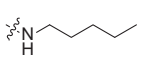 | **50–200** | **64.4 ± 8.2** | > 200 | > 200 | **18.0 ± 0.6** | > 200 |
| 4 | 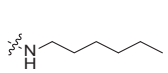 | **50–200** | **50–200** | > 200 | > 200 | **3.14 ± 1.20** | > 200 |
| 5 | 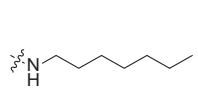 | > 200 | > 200 | > 200 | > 200 | **0.77 ± 0.04** | > 200 |
| 6 | 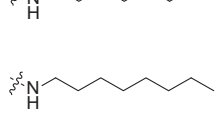 | > 200 | > 200 | > 200 | > 200 | **0.74 ± 0.17** | > 200 |
| 7 |  | > 200 | > 200 | > 200 | > 200 | **50–200** | > 200 |
| 8 |  | > 200 | > 200 | > 200 | > 200 | **50–200** | > 200 |
| 9 |  | **101 ± 3** | > 200 | > 200 | **50–200** | **34.7 ± 4.2** | > 200 |
| 10 |  | > 200 | > 200 | > 200 | > 200 | > 200 | > 200 |
| 11 |  | **50–200** | > 200 | > 200 | > 200 | **50–200** | > 200 |
| 12 |  | **55.3 ± 0.8** | > 200 | > 200 | > 200 | **22.3 ± 1.8** | > 200 |
| 13 |  | > 200 | > 200 | > 200 | > 200 | **50–200** | > 200 |
| 14 |  | **136 ± 26** | > 200 | > 200 | > 200 | **24.7 ± 0.3** | > 200 |

**Table 1.** (Continued).

| PanAm entry | $R_{Am}$ group | *E. coli* MIC (μM) | | | *S. aureus* MIC (μM) | | |
|---|---|---|---|---|---|---|---|
| | | α-PanAm | *n*-PanAm | HoPanAm | α-PanAm | *n*-PanAm | HoPanAm |
| 15 | 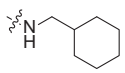 | > 200 | > 200 | > 200 | > 200 | **50–200** | > 200 |
| 16 | 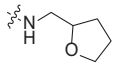 | > 200 | > 200 | > 200 | > 200 | **50–200** | > 200 |
| 17 | 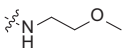 | > 200 | > 200 | > 200 | > 200 | > 200 | > 200 |
| 18 | 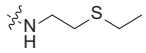 | **50–200** | > 200 | > 200 | > 200 | **50–200** | > 200 |
| 19 | 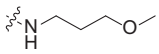 | > 200 | > 200 | > 200 | > 200 | > 200 | > 200 |
| 20 | 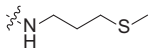 | **50–200** | **50–200** | > 200 | > 200 | **50–200** | > 200 |
| 21 | 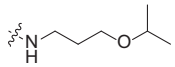 | > 200 | > 200 | > 200 | > 200 | **50–200** | > 200 |
| 22 | 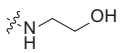 | > 200 | > 200 | > 200 | > 200 | > 200 | > 200 |
| 23 | 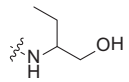 | > 200 | > 200 | > 200 | > 200 | **50–200** | > 200 |
| 24 | 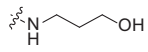 | > 200 | > 200 | > 200 | **50–200** | > 200 | > 200 |
| 25 | 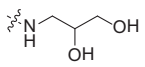 | > 200 | > 200 | > 200 | > 200 | > 200 | > 200 |
| 26 | 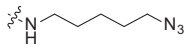 | > 200 | > 200 | > 200 | > 200 | **50–200** | > 200 |
| 27 | 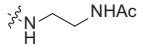 | > 200 | > 200 | > 200 | > 200 | > 200 | > 200 |

**Table 1.** (Continued).

| PanAm entry | $R_{Am}$ group | *E. coli* MIC (μM) | | | *S. aureus* MIC (μM) | | |
|---|---|---|---|---|---|---|---|
| | | α-PanAm | *n*-PanAm | HoPanAm | α-PanAm | *n*-PanAm | HoPanAm |
| 28 | 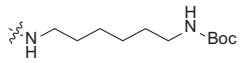 | > 200 | > 200 | > 200 | > 200 | > 200 | > 200 |
| 29 | 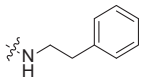 | > 200 | > 200 | > 200 | > 200 | **47.7 ± 7.9** | > 200 |
| 30 | 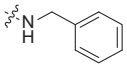 | > 200 | > 200 | > 200 | > 200 | > 200 | > 200 |
| 31 | 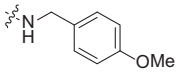 | > 200 | > 200 | > 200 | > 200 | > 200 | > 200 |
| 32 | 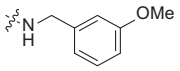 | > 200 | > 200 | > 200 | > 200 | **55.0 ± 10.2** | > 200 |
| 33 | 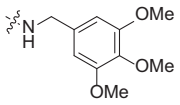 | > 200 | > 200 | > 200 | > 200 | > 200 | > 200 |
| 34 | 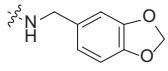 | > 200 | > 200 | > 200 | > 200 | **50–200** | > 200 |
| 35 | 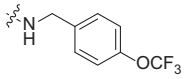 | > 200 | > 200 | > 200 | > 200 | > 200 | > 200 |
| 36 | 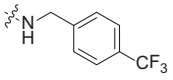 | > 200 | > 200 | > 200 | > 200 | > 200 | > 200 |
| 37 | 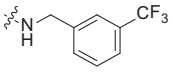 | > 200 | > 200 | > 200 | > 200 | > 200 | > 200 |
| 38 | 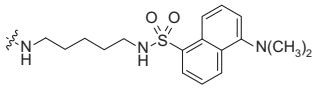 | > 200 | > 200 | > 200 | > 200 | > 200 | > 200 |
| 39 |  | > 200 | > 200 | > 200 | > 200 | > 200 | > 200 |

**Table 1.** (Continued).

| PanAm entry | $R_{Am}$ group | *E. coli* MIC (μM) | | | *S. aureus* MIC (μM) | | |
|---|---|---|---|---|---|---|---|
| | | α-PanAm | *n*-PanAm | HoPanAm | α-PanAm | *n*-PanAm | HoPanAm |
| 40 |  | > 200 | > 200 | > 200 | > 200 | > 200 | > 200 |
| 41 | 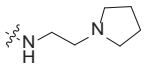 | > 200 | > 200 | > 200 | > 200 | > 200 | > 200 |
| 42 | 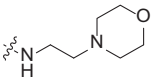 | > 200 | > 200 | > 200 | > 200 | > 200 | > 200 |
| 43 | 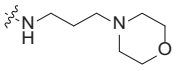 | > 200 | > 200 | > 200 | > 200 | > 200 | > 200 |
| 44 | 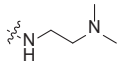 | > 200 | > 200 | > 200 | > 200 | > 200 | > 200 |
| 45 | 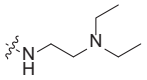 | > 200 | > 200 | > 200 | > 200 | > 200 | > 200 |
| 46 | 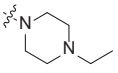 | > 200 | > 200 | > 200 | > 200 | > 200 | > 200 |
| 47 | 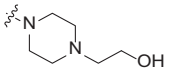 | > 200 | > 200 | > 200 | > 200 | > 200 | > 200 |

tested are given in Table 1. Importantly, the data obtained for the *n*-PanAm set correlate well with the results of previous pantothenamide structure–activity relationship studies, with the MIC values differing by no more than 10-fold (some differences are expected due to variation in the amount of Pan present in tryptone) [8,14,15].

Comparative analysis of the results indicated that *E. coli* was only inhibited by a small number of α-PanAm and *n*-PanAm series members, most of which had MIC values in the 50–100 μM range. Previous studies have demonstrated that, at least in some cases (such as with *n*-PanAm-5, otherwise known as *N*-heptyl pantothenamide or N7-Pan), this relatively poor inhibition profile can be ascribed to TolC-dependent efflux because TolC-defective strains do show sensitivity [8,15]. By contrast, *S. aureus* was only inhibited by *n*-PanAm compounds. These showed MIC values that varied by almost two orders of magnitude, with the best inhibitors (*n*-PanAm-5/N7-Pan and *n*-PanAm-6) having MIC values of ~ 0.7 μM. As expected, *P. aeruginosa* showed no inhibition by any of the pantothenamides tested, including the smaller sized α-PanAm series.

## Pantothenamide-mediated growth inhibition correlates with PanK activity in *E. coli* but not *S. aureus*

Next, we investigated whether the differences in the *E. coli* and *S. aureus* growth inhibition profiles could

be correlated with the activity and/or selectivity of their respective PanKs. The pantothenamides that showed the most potent growth inhibition were tested as substrates of the purified overexpressed enzymes at a fixed concentration (100 μM) using an established pyruvate kinase/lactate dehydrogenase (PK/LDH)-based coupled enzyme assay that links ADP production to the consumption of NADH [7]. Although this assay measures the enzymes' activity indirectly, it has been shown previously that the expected monophosphorylated ester is produced and that the PK/LDH-assay is a viable alternative for measuring PanK activity [7,13,21,31]. The corresponding compounds that have the same amide substituent but different substitutions of the β-alanine moiety were included for comparison. The data indicate that, for *Ec*PanK$_I$, compounds that show growth inhibition belong to the α- and *n*-PanAm series and have specific activities very similar to that measured for Pan, whereas the HoPanAms, which do not inhibit *E. coli* growth, show poor PanK activity (Fig. 2A). However, PanK activity is not necessarily a predictor of growth inhibition because even α- and *n*-PanAm compounds that do not show growth inhibition still show similar specific activity levels. Unexpectedly, the situation is reversed in *S. aureus*, with only the non-inhibitory HoPanAm members showing *S. aureus* type II PanK (*Sa*PanK$_{II}$) activity approaching that seen for Pan (Fig. 2B).

To further investigate these differences and their relevance to the pantothenamide mode of action, kinetic profiles were obtained for both enzymes with Pan and the three pantothenamides with *N*-pentyl substituents [i.e. α-PanAm-3, *n*-PanAm-3 (referred to as N5-Pan from here on) and HoPanAm-3] (Fig. 2C). These confirm that the pantothenamides that acted as *E. coli* inhibitors (N5-Pan and α-PanAm-3) have *Ec*PanK$_I$ activity profiles that closely resemble that of Pan. HoPanAm-3, which did not act as an *E. coli* growth inhibitor, is clearly a poor *Ec*PanK$_I$ substrate. By contrast, the *S. aureus* growth inhibitor N5-Pan has a very different activity profile that shows both a lower apparent $K_m$ ($K_m^{app}$) and significantly reduced turnover compared to Pan (Fig. 2D). The two pantothenamides that did not show inhibition of *S. aureus*, α-PanAm-3 and HoPanAm-3, are apparently poor and excellent substrates, respectively.

To confirm these trends, we extended the studies to other selected growth inhibitory pantothenamides. We found that *Ec*PanK$_I$ also accepts α-PanAm-12 and α-PanAm-14 as substrates (Fig. 2E), whereas *Sa*PanK$_{II}$ shows the same unusual kinetic profile for *n*-PanAm-5, *n*-PanAm-9, *n*-PanAm-12 and *n*-PanAm-29 that combines a low $K_m^{app}$ with low turnover (Fig. 2F). Among these compounds, *n*-PanAm-5 (N7-Pan) showed the lowest turnover; importantly, it is also the pantothenamide that exhibits the most potent growth inhibition of *S. aureus* identified to date [13,14]. These results strongly suggest that in *E. coli* PanK activity is a necessary (but not sufficient) requirement for pantothenamides to show growth inhibition. By contrast, pantothenamides that show growth inhibition of *S. aureus* bind its PanK enzyme with high apparent affinity, yet show poor turnover.

## Quantifying the variations in PanK kinetics: constructing a kinetic model

Several previous studies have used the Michaelis–Menten equation to obtain kinetic parameters for both *Ec*PanK$_I$ and *Sa*PanK$_{II}$ acting on a range of substrates [7,13,14,16,32–34]. In the present study we took special care to obtain all measurements during the initial phase of the reaction (< 10% substrate consumed), and found that *Ec*PanK$_I$ has a hyperbolic activity profile only for Pan, whereas it shows sigmoidal saturation curves for the pantothenamides (Fig. 3A). *Sa*PanK$_{II}$ has sigmoidal saturation curves for both Pan and HoPanAm-3 (the low $K_m^{app}$ for N5-Pan limited our ability to determine if this is also true in its case). These findings indicate that some substrates have a positive cooperative effect on PanK catalysis, a phenomenon that has previously only been described for certain PanK$_{III}$s [35].

The sigmoidal saturation data were best described by a simple Hill-type equation (Eqn 1) derived according to a mechanism based on a dimeric enzyme with one active site per subunit; the available structural data shows that both *Ec*PanK$_I$ and *Sa*PanK$_{II}$ conform to this description [20,26,36]. This mechanism, shown schematically for *Sa*PanK$_{II}$ acting on Pan in Fig. 3B, is based on the assumption that only enzyme states with both of the active sites occupied (e.g. $E_{Pan.Pan}$) have to be considered and lead to product formation (as is usually the case for cooperative enzymes). The differential binding of the substrate to the two active sites is described by the parameter α that modifies the dissociation constant for the enzyme form with substrate bound in both active sites. In Eqn (1), $k_f$ denotes the rate of transformation (phosphorylation) of Pan, $E_T$ is the total enzyme concentration and $K_{Pan}$ is the dissociation

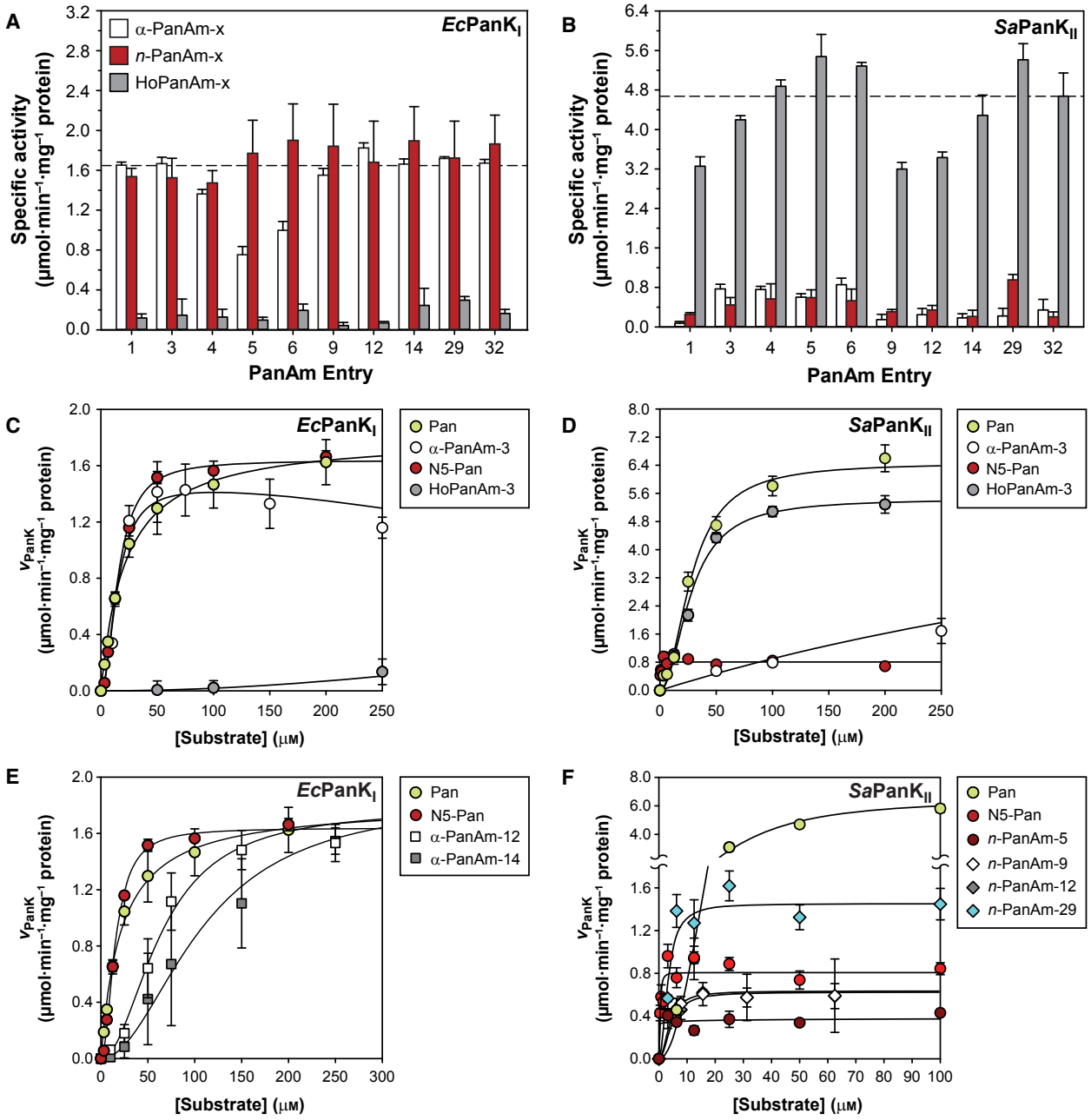


**Fig. 2.** Activity of *Ec*PanK$_I$ and *Sa*PanK$_{II}$ towards selected pantothenamides. (A) The specific activities for *Ec*PanK$_I$ towards Pan (dashed line) and the pantothenamides (bars) at 100 μM. The data were obtained from a single experiment performed in triplicate; the error bars denote the SD. (B) The data for *Sa*PanK$_{II}$ against Pan (dashed line) and the same panel of pantothenamides (bars). (C) Activity profiles for *Ec*PanK$_I$ with Pan, α-PanAm-3, N5-Pan and HoPanAm-3 as substrates. For information on statistical analysis and equations used to fit the data, see Table 2. (D) As for (C) but with *Sa*PanK$_{II}$. (E) *Ec*PanK$_I$ activity profiles with the *E. coli* growth inhibitory pantothenamides N5-Pan, α-PanAm-12 and α-PanAm-14 as substrates, with the Pan profile shown for comparison. Description and data analysis is as indicated for (C). (F) *Sa*PanK$_{II}$ activity profiles of the *S. aureus* growth inhibitory pantothenamides N5-Pan, *n*-PanAm-5 (N7-Pan), *n*-PanAm-9, *n*-PanAm-12 and *n*-PanAm-29, with the Pan profile shown for comparison. Note the *y*-axis break. Description and data analysis is as indicated for (C).

constant of Pan; $V_{max}$ is then equal to $2{\cdot}k_f{\cdot}E_T$, and $K_{0.5}^{Pan}$ (the $K_{0.5}$ value for Pan) is numerically equal to the concentration of Pan where $v_{PanK} = 0.5{\cdot}V_{max}$. Note that, from these conditions, it follows that $K_{Pan} = \sqrt{\alpha \cdot (K_{0.5}^{Pan})^2}$.

$$v_{\mathrm{PanK}} = 2 \cdot k_f \cdot [E_{\mathrm{Pan\cdot Pan}}] = \frac{2 \cdot k_f \cdot E_T \cdot \alpha \left(\frac{[\mathrm{Pan}]}{K_{\mathrm{Pan}}}\right)^2}{1 + \alpha \cdot \left(\frac{[\mathrm{Pan}]}{K_{\mathrm{Pan}}}\right)^2} = \frac{V_{\max} \cdot \left(\frac{[\mathrm{Pan}]}{K_{0.5}^{\mathrm{Pan}}}\right)^2}{1 + \left(\frac{[\mathrm{Pan}]}{K_{0.5}^{\mathrm{Pan}}}\right)^2} \quad (1)$$

Fitting Eqn (1) to the saturation data showed a good fit in all cases, as exemplified by the curve of *Sa*PanK$_{II}$ with Pan (Fig. 3C), and allowed determination of the relevant kinetic parameters. These values, summarized in Table 2, indicate that although for *E. coli* there is general agreement between a pantothenamide's growth inhibitory potency and the specific activity that *Ec*PanK$_I$ shows towards it, there is no direct correlation, as would be expected if the enzyme merely served as a gateway for the metabolic activation of these compounds, which subsequently have their inhibitory effect elsewhere. For *S. aureus*, potency correlates with compounds that have the unusual combination of very low (< 5 μM) values of $K_{0.5}$ and low turnover rates, and, consequently, very high apparent specificity constants ($k_{cat}/K_{0.5}$).

## N5-Pan has an inhibitory binding interaction with *Sa*PanK$_{II}$ but not with *Ec*PanK$_I$

To further investigate the importance of the activity profile differences, we obtained kinetic profiles for both enzymes acting on mixtures of Pan and N5-Pan; this pantothenamide was chosen for this particular experiment because it inhibits both *E. coli* and *S. aureus* growth and therefore allows for a comparative analysis. For each experiment, the total substrate concentration was increased at the same time as maintaining a constant ratio of Pan:N5-Pan; in subsequent experiments, the amount of Pan in the ratio was increased in a stepwise manner, from 0% (pure N5-Pan) to 100% (pure Pan). The combined turnover of Pan and N5-Pan was measured using the PK/LDH-based assay that responds to the formation of ADP.

The results demonstrate that, for *Ec*PanK$_I$, the resulting activity profiles show very small differences, and that there is a gradual progression from the profile for Pan to that for N5-Pan (Fig. 4A). However, for *Sa*PanK$_{II}$, even small amounts (i.e. 5%) of N5-Pan exert both an inhibitory effect (at mixture concentrations of 50 μM and higher) and an apparent stimulatory effect (at mixture concentrations of ~ 12.5 μM and below) on activity (Fig. 4B). Overall, the impact of N5-Pan on *Sa*PanK$_{II}$ activity is unexpectedly complex. In comparison, mixtures of Pan and HoPanAm-3, which acts as a substrate of *Sa*PanK$_{II}$ but does not show *S. aureus* growth inhibition, yielded essentially the same kinetic profile regardless of the composition of the substrate mixture (Fig. 4C). These results confirm that pantothenamides that show growth inhibition in

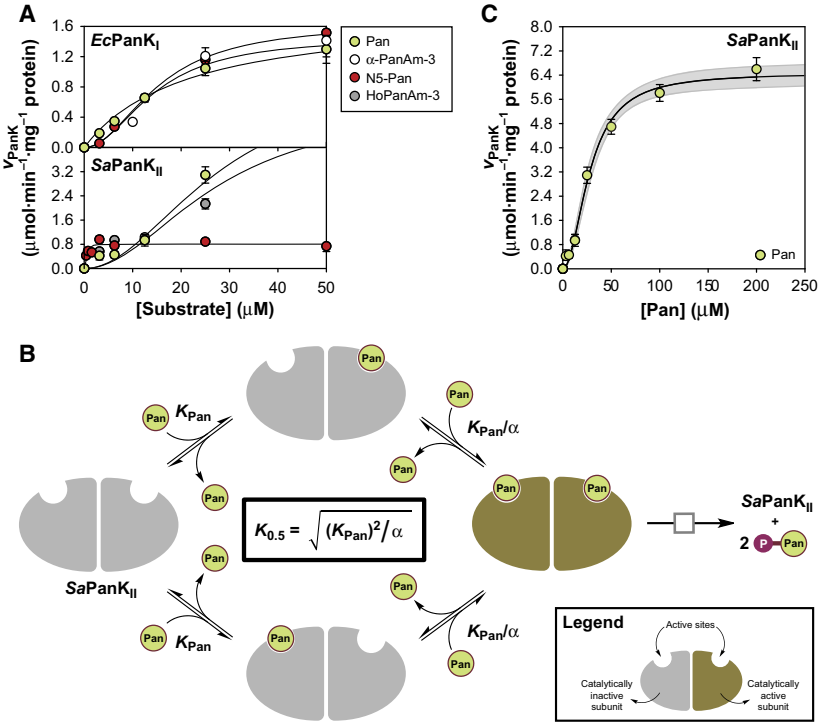


**Fig. 3.** Constructing a kinetic model for *Sa*PanK$_{II}$ activity. (A) Activity profiles for *Ec*PanK$_I$ and *Sa*PanK$_{II}$ shown in Fig. 2C,D at low substrate concentration to highlight the sigmoidal nature of the curves. (B) Schematic representation of the *Sa*PanK$_{II}$ kinetic model, based on an enzyme with two subunits, from which Eqn (1) is derived. $K_{Pan}$ is the dissociation constant of Pan, and α denotes the change in dissociation constant in the enzyme form with Pan bound to both subunits. This is the active form of the enzyme (shown in green), which catalyzes the phosphorylation reaction as denoted by the arrow with the open square. (C) Fitting Eqn (1) to the data points for the activity of *Sa*PanK$_{II}$ towards Pan, with the line indicating the best fit and the shaded area showing the 90% confidence interval. Parameter values and SEs are given in Table 2.

*S. aureus* have multifaceted interactions with its PanK enzyme, and that they do not simply act as alternative substrates.

### DL-4′-Deoxy-N5-Pan acts as an inhibitor of *Sa*PanK$_{II}$ turnover and *S. aureus* growth

To simplify the analysis of the interaction of N5-Pan with *Sa*PanK$_{II}$, we prepared its structural analogue DL-4′-deoxy-*N*-pentylpantothenamide (dN5) by $NaBH_4$-mediated reduction of a ketoamide precursor, to give the product as the racemate (Fig. 5A). This compound is expected to exclusively act as an inhibitor because it has the 4′-OH group of N5-Pan removed, thereby preventing it from being a PanK substrate (although all other binding interactions are retained).

Experiments were performed on both *Ec*PanK$_I$ and *Sa*PanK$_{II}$ using reaction mixtures that contained 25 μM Pan and increasing concentrations of either N5-Pan or dN5. The addition of N5-Pan increased the total observed activity for *Ec*PanK$_I$ as expected for an alternate substrate, whereas dN5 acted as a very poor inhibitor of the enzyme ($IC_{50}$ ~ 500 μM) (Fig. 5B). Full kinetic analysis subsequently indicated that this is the result of a minor reduction of the $V_{max}^{app}$ (data not shown), confirming that the 4′-OH group is an important determinant for ligand binding in *Ec*PanK$_I$ [26].

By contrast, both N5-Pan and dN5 showed the same apparent inhibitory effect on *Sa*PanK$_{II}$ with $IC_{50}$ values of 4.8 ± 1.2 and 7.3 ± 0.9 μM, respectively (Fig. 5C). For this enzyme, full kinetic analysis again showed a dual effect (Fig. 5D), with dN5 causing a small but significant reduction in the $K_{0.5}^{app}$ for Pan and a large reduction in the $V_{max}^{app}$. Additionally, growth inhibition tests performed in minimal medium showed that dN5 has a MIC of ~ 50 μM for *S. aureus* but does not inhibit *E. coli* (Fig. 6). By comparison, N5-Pan still has a much lower MIC (approximately 1.5 μM) for *S. aureus* under these conditions. Nonetheless, this result unambiguously shows that even pantothenamide analogues unable to act as PanK substrates have a negative impact on *S. aureus* growth.

### Expanding the kinetic model to account for complex interaction of N5-Pan with *Sa*PanK$_{II}$

We next used the dN5 data to expand the kinetic model for *Sa*PanK$_{II}$ to include a mechanism that could account for the dual stimulatory/inhibitory effect exerted by both dN5 and N5-Pan. Because the N5-Pan saturation kinetics did not show substrate inhibition at high concentrations, we started with an uncompetitive inhibition mechanism for dN5 [i.e. one in which it only binds to the *Sa*PanK$_{II}$–Pan ([$E_{Pan}$]) complex]. In addition, we also included a competitive inhibition mechanism in which dN5 can bind to any unoccupied active site. This led to the mechanistic scheme shown in Fig. 7A, which can be translated into a rate equation that assumes that only the [$E_{Pan.Pan}$], [$E_{Pan.dN5}$] and [$E_{dN5.Pan}$] complexes have catalytic activity, and in which no enzyme form that has only one active site occupied is considered (Eqn 2). The parameters in this equation are defined as those used in Eqn (1), with the addition of $K_{dN5}$ (dissociation constant for the competitive inhibition by dN5) and $K_{dN5'}$ (dissociation constant for the uncompetitive inhibition by dN5): Equation (2) was able to describe the data very well (Fig. 5D, solid lines) and accounted for both the stimulatory effect of the inhibitor at low substrate concentrations and the reduction in $V_{max}^{app}$ at high substrate concentrations. These effects are based on the dissociation constants for the binding of dN5 in a competitive ($K_{dN5}$ = 3.81 ± 0.45 μM) and uncompetitive ($K_{dN5'}$ = 41.0 ± 7.1 μM) binding mode, respectively, which clearly show that, for dN5, the former is the stronger interaction (Table 3). Additionally, the dissociation constant for Pan ($K_{Pan}$ = 9.31 ± 0.70 μM) and the value for α (0.111 ± 0.017 μM) were also calculated in this manner. The $K_{0.5}$ value of 27.9 μM calculated from these values is almost identical to the value of 27.8 μM obtained by fitting Eqn 1 to the Pan activity profile (Fig. 3C and Table 2).

The newly expanded mechanism can easily account for the data obtained from *Sa*PanK$_{II}$ acting on mixtures of Pan and N5-Pan (Fig. 4B) by modifying the competitive inhibition component exerted by dN5 to that of a competitive substrate with catalytic turnover. This confers activity on the two boxed complexes in

$$v_{PanK} = 2 \cdot k_f \cdot [E_{Pan \cdot Pan}] + 2 \cdot k_f \cdot [E_{Pan \cdot dN5}] = \frac{V_{max} \cdot \left(\frac{[Pan]}{K_{Pan}}\right) \cdot \left(\alpha \cdot \frac{[Pan]}{K_{Pan}} + \frac{[dN5]}{K_{dN5}}\right)}{1 + \alpha \cdot \left(\frac{[Pan]}{K_{Pan}}\right)^2 \cdot \left(1 + \left(\frac{[dN5]}{K_{dN5'}}\right)^2\right) + 2 \cdot \left(\frac{[Pan] \cdot [dN5]}{K_{Pan} \cdot K_{dN5}}\right) \cdot \left(1 + \frac{[dN5]}{K_{dN5'}}\right) + \left(\frac{[dN5]}{K_{dN5}}\right)^2} \quad (2)$$

**Table 2.** PanK kinetic parameters with Pan and various pantothenamides. Kinetic parameters were determined by keeping the ATP concentration constant at 1.5 mM in all cases. All reported parameters are the mean of those obtained by fitting the given equation to the data obtained for each individual experiments; the error values represent the range/2 (for parameters obtained from two independent experiments) or SEM (for parameters obtained from three or more independent experiments). References to compounds tested in previous studies are provided in the main text. ND, not determined.

| | *Ec*PanK$_I$ | | | | | | *Sa*PanK$_{II}$ | | | | | |
|---|---|---|---|---|---|---|---|---|---|---|---|---|
| Compound | $K_{0.5}$[a] (μM) | $k_{cat}$ ($s^{-1}$) | $k_{cat}/K_{0.5}$[a] ($mM^{-1}\cdot s^{-1}$) | $N$[b] | Equation fitted | $R^2$ value[c] | $K_{0.5}$ (μM) | $k_{cat}$ ($s^{-1}$) | $k_{cat}/K_{0.5}$ ($mM^{-1}\cdot s^{-1}$) | $N$[b] | Equation fitted | $R^2$ value[c] |
| Pan | 21.3 ± 1.4 | 1.16 ± 0.14 | 54.5 ± 3.1 | 2 | Michaelis–Menten | 0.9955 | 27.8 ± 3.3 | 3.37 ± 0.24 | 124 ± 7 | 4 | Eqn (1) | 0.9928 |
| α-PanAm-3 | 14.6 ± 1.1 | 0.95 ± 0.13 | 64.3 ± 4.3 | 2 | Modified Eqn (1)[d] | 0.9679 | 783 ± 64 | 4.14 ± 0.14 | 5.29 ± 0.62 | 1[e] | Michaelis–Menten | 0.8719 |
| *n*-PanAm-3 [N5-Pan] | 15.6 ± 1.2 | 1.06 ± 0.03 | 68.6 ± 3.4 | 2 | Eqn (1) | 0.9988 | < 1.5[f] | 0.44 ± 0.03 | > 290 | 4 | Eqn (1) | 0.8606 |
| HoPanAm-3 | 720 ± 95 | 0.62 ± 0.04 | 0.87 ± 0.17 | 1[e] | Eqn (1) | 0.8866 | 27.8 ± 2.3 | 2.85 ± 0.11 | 103 ± 6 | 3 | Eqn (1) | 0.9740 |
| α-PanAm-12 | 63 ± 11 | 1.05 ± 0.12 | 18.2 ± 4.3 | 3 | Eqn (1) | 0.9881 | ND | | | | | |
| α-PanAm-14 | 151 ± 56 | 1.37 ± 0.15 | 13.8 ± 6.6 | 3 | Eqn (1) | 0.9911 | ND | | | | | |
| *n*-PanAm-5 [N7-Pan] | ND | | | | | | 2.04 ± 0.54 | 0.22 ± 0.02 | 118 ± 41 | 2 | Eqn (1) | 0.8677 |
| *n*-PanAm-9 | ND | | | | | | 4.94 ± 0.94 | 0.33 ± 0.12 | 65.4 ± 11.8 | 2 | Eqn (1) | 0.9711 |
| *n*-PanAm-12 | ND | | | | | | 4.47 ± 0.11 | 0.32 ± 0.04 | 72.7 ± 10.0 | 2 | Eqn (1) | 0.9326 |
| *n*-PanAm-29 | ND | | | | | | 3.49 ± 0.50 | 0.75 ± 0.06 | 232 ± 59 | 3 | Eqn (1) | 0.9326 |
| PantSH | 23.6 ± 2.1 | 1.00 ± 0.09 | 42.4 ± 0.3 | 3 | Michaelis–Menten | 0.9949 | < 1.5[f] | 0.39 ± 0.09 | > 260 | 4 | Eqn (1) | 0.8714 |

[a] In those cases where the Michaelis–Menten equation was used to fit the data, $K_{0.5}$ is $K_m$.

[b] Number of independent experiments.

[c] $R^2$ value for the indicated equation fitted to the data averaged from all the experiments.

[d] α-PanAm-3 showed inhibition of *Ec*PanK$_I$ at high substrate concentrations; using a modified version of Eqn (1) that accounts for the uncompetitive substrate inhibition, a $K_i$ of 720 ± 120 μM was determined.

[e] As a result of the high $K_{0.5}$ value, kinetic parameters were determined by fitting the equation to the data from a single experiment performed in triplicate; errors indicate the SE of the fit.

[f] The low $K_{0.5}^{app}$ values of these compounds cannot be reported with accuracy because they fall below the sensitivity limit of the assay.

Fig. 7A as shown in Fig. 7B, and gives the corresponding rate equation Eqn (3) that was fitted to the Pan/N5-Pan experimental data, constraining the values for $V_{max}^{Pan}$ (the $V_{max}$ for Pan), $K_{Pan}$ and α to those obtained before. In this equation, $k_f^{Pan}$ and $k_f^{N5\text{-}Pan}$ denote the rates of phosphorylation of Pan and N5-Pan respectively, giving $V_{max}^{Pan} = 2 \cdot k_f^{Pan} \cdot E_T$ for Pan and $V_{max}^{N5\text{-}Pan} = 2 \cdot k_f^{N5\text{-}Pan} \cdot E_T$ for N5-Pan. Additionally, $K_{N5\text{-}Pan}$ is the dissociation constant of N5-Pan acting as a substrate, whereas $K_{N5\text{-}Pan'}$ is the dissociation constant for the uncompetitive inhibition component that it exerts:

The equation provided a very good description of the experimental data set (Fig. 8A) and gave the parameter values listed in Table 3. These indicate that, although the dissociation constant of N5-Pan for binding at the active site (i.e. as a substrate) is similar to that of dN5 ($K_{N5\text{-}Pan}$ = 2.22 ± 0.48 μM), its dissociation constant for binding as an uncompetitive inhibitor ($K_{N5\text{-}Pan'}$ = 4.89 ± 0.66 μM) is much smaller. Because N5-Pan also has a much reduced MIC compared to dN5, this provides additional evidence for the uncompetitive inhibition of *Sa*PanK$_{II}$ as an important contributor to the inhibition of *S. aureus* growth by N5-Pan.

$$\begin{aligned} v_{PanK} &= 2 \cdot k_f^{Pan} \cdot [E_{Pan\cdot Pan}] + 2 \cdot k_f^{Pan} \cdot [E_{Pan\cdot N5\text{-}Pan}] + 2 \cdot k_f^{N5\text{-}Pan} \cdot [E_{N5\text{-}Pan\cdot N5\text{-}Pan}] + 2 \cdot k_f^{N5\text{-}Pan} \cdot [E_{N5\text{-}Pan\cdot Pan}] \\ &\quad + 2 \cdot k_f^{N5\text{-}Pan} \cdot [E_{N5\text{-}Pan\cdot Pan}^{N5\text{-}Pan}] \\ &= \frac{V_{max}^{Pan} \cdot \left(\frac{[Pan]}{K_{Pan}}\right) \cdot \left(\alpha \cdot \frac{[Pan]}{K_{Pan}} + \frac{[N5\text{-}Pan]}{K_{N5\text{-}Pan}}\right) + V_{max}^{N5\text{-}Pan} \cdot \left(\frac{[N5\text{-}Pan]}{K_{N5\text{-}Pan}}\right) \cdot \left(\frac{[N5\text{-}Pan]}{K_{N5\text{-}Pan}} + \frac{[Pan]}{K_{Pan}} + \left(1 + \frac{[N5\text{-}Pan]}{K_{N5\text{-}Pan'}}\right)\right)}{1 + \alpha \cdot \left(\frac{[Pan]}{K_{Pan}}\right)^2 \cdot \left(1 + \left(\frac{[N5\text{-}Pan]}{K_{N5\text{-}Pan'}}\right)^2\right) + 2 \cdot \left(\frac{[Pan]\cdot[N5\text{-}Pan]}{K_{Pan}\cdot K_{N5\text{-}Pan}}\right) \cdot \left(1 + \frac{[N5\text{-}Pan]}{K_{N5\text{-}Pan'}}\right) + \left(\frac{[N5\text{-}Pan]}{K_{N5\text{-}Pan}}\right)^2} \end{aligned} \quad (3)$$

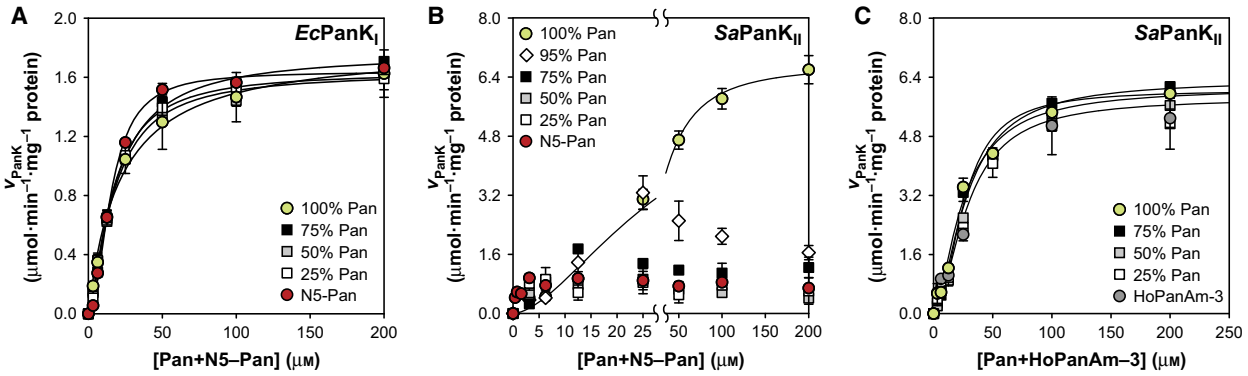


**Fig. 4.** Analyzing the interaction of Pan and N5-Pan with *Ec*PanK$_I$ and *Sa*PanK$_{II}$ under competitive conditions. (A) Kinetic profiles of mixtures of Pan and N5-Pan determined with *Ec*PanK$_I$. The *x*-axis indicates the total substrate concentration (Pan and N5-Pan combined); for each data set, the ratio of Pan:N5-Pan was kept at a constant value. The data points represent the mean of two independent experiments, each performed in triplicate; the error bars denote the range/2. Because the curves progress from a hyperbolic to a sigmoidal shape, the solid lines represent the best fit of the data to the Hill equation with the value for *h* (Hill coefficient) constrained to between 1 and 2. (B) Kinetic profiles of mixtures of Pan and N5-Pan determined with *Sa*PanK$_{II}$ as described for (A). The solid line represents the best fit of Eqn (1) to the 100% Pan data. (C) Kinetic profiles of mixtures of Pan and HoPanAm-3 determined for *Sa*PanK$_{II}$ as described for (A).

In the absence of Pan, Eqn (3) reduces to a much simpler form (Eqn 4), which describes the saturation kinetics of inhibitory pantothenamides such as N5-Pan.

$$v_{\mathrm{PanK}} = 2 \cdot k_f^{\mathrm{N5\text{-}Pan}} \cdot [E_{\mathrm{N5-Pan\cdot N5\text{-}Pan}}] = \frac{V_{\mathrm{max}}^{\mathrm{N5-Pan}} \cdot \left(\frac{[\mathrm{N5\text{-}Pan}]}{K_{\mathrm{N5\text{-}Pan}}}\right)^2}{1 + \left(\frac{[\mathrm{N5\text{-}Pan}]}{K_{\mathrm{N5\text{-}Pan}}}\right)^2} \quad (4)$$

This equation is equivalent to Eqn (1), which was used to obtain the parameters shown in Table 2, if $K_{0.5} = K_{\mathrm{Pan}}$ (i.e. if $\alpha = 1$). This would indicate that there is no differentiation in the binding of N5-Pan to the enzyme's two active sites.

## *Sa*PanK$_{II}$ atypical kinetic mechanism follows from its role in CoA salvage biosynthesis

The question arises as to why there is such a selective binding site in *Sa*PanK$_{II}$ that it accepts N5-Pan at the same time as excluding HoPanAm-3 (note that the latter did not show any uncompetitive inhibition mode; Fig. 4C). Clearly, the selectivity is for compounds that contain the natural β-alanine moiety, suggesting that the site is predisposed to bind compounds containing the native pantothenoyl group. Based on its close structural similarity to *n*-PanAm series compounds (such as N5-Pan), we considered PantSH (the substrate of the CoA salvage pathway; Fig. 1A) as the most likely natural ligand for this binding site.

To test such a hypothesis, we measured the activity of *Ec*PanK$_I$ and *Sa*PanK$_{II}$ against mixtures that contained 25 μM Pan and increasing concentrations of PantSH. The results are strikingly similar to those obtained for N5-Pan, with PantSH increasing the total observed activity for *Ec*PanK$_I$ but inhibiting *Sa*PanK$_{II}$ activity (Fig. 8B). Similarly, when constant ratio mixtures of Pan and PantSH were analyzed as conducted for N5-Pan, the profiles clearly demonstrate that PantSH has the same complex interaction with *Sa*PanK$_{II}$ (Fig. 8C), showing both a stimulatory (at low concentrations) and an inhibitory (at high concentrations) effect on turnover that is even more pronounced than that caused by N5-Pan. Based on the similarity between N5-Pan and PantSH, Eqn (3) was used to describe the Pan/PantSH experimental data by substituting PantSH for N5-Pan, and again constraining the $V_{\mathrm{max}}^{\mathrm{app}}$, $K_{\mathrm{Pan}}$ and α values to those obtained previously. The equation was able to describe the experimental data set well (Fig. 8C), and gave values for $K_{\mathrm{PantSH}}$ (binding at the active site, i.e. as substrate) and $K_{\mathrm{PantSH'}}$ (binding in an uncompetitive mode) of $0.46 \pm 0.08$ μM and $6.03 \pm 1.27$ μM, respectively (Table 3). In comparison with the values obtained for N5-Pan, PantSH appears to be the better substrate at the same time as showing similar uncompetitive inhibition to N5-Pan. Consequently, PantSH is more effective at activating *Sa*PanK$_{II}$ at low substrate concentrations (Fig. 8A,C, insets). Interestingly, when the activity of *Sa*PanK$_{II}$ activity against constant ratio mixtures of Pan and *n*-PanAm-5 (N7-Pan, the most potent *S. aureus* growth inhibitor) was measured and analyzed in a similar manner, the obtained kinetic parameters were almost identical to those found for PantSH (data not shown). Taken together, these results strongly suggest that pantothenamides showing

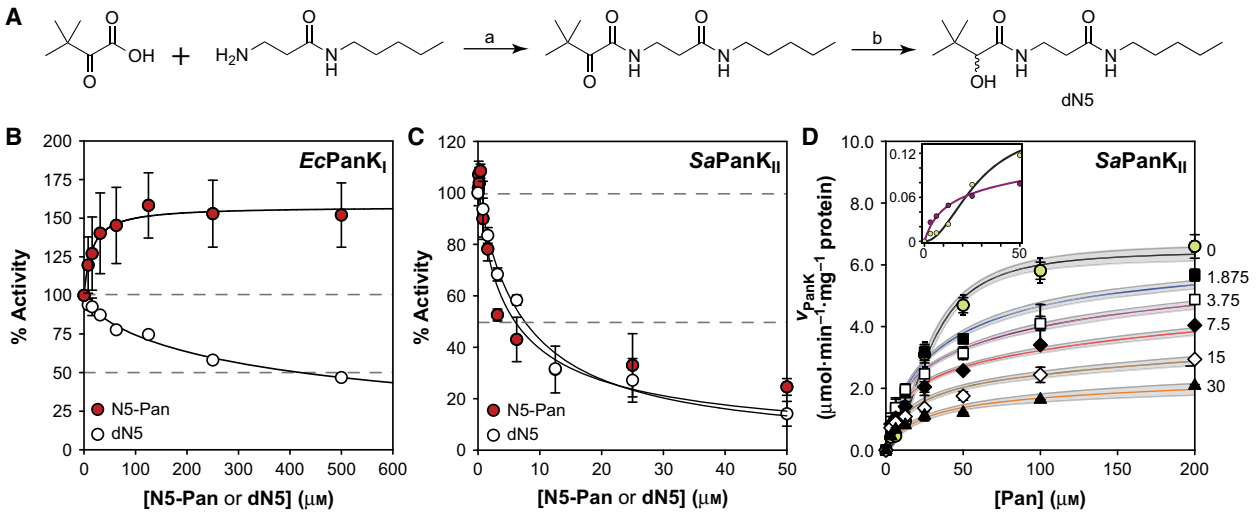


**Fig. 5.** dN5 as a PanK inhibitor. (A) Synthetic scheme for the preparation of dN5. (a) 1-Ethyl-3-(3-dimethylaminopropyl) carbodiimide hydrochloride (EDC), hydroxybenzotriazole (HOBt), *N,N*-diisopropylethylamine (DIPEA), $CH_2Cl_2$; (b) $NaBH_4$, methanol. (B) Activity/inhibition profiles for *Ec*PanK$_I$ when treated with N5-Pan and dN5 at a fixed concentration of 25 μM Pan. The data points represent the mean of two independent experiments, each performed in triplicate; the error bars denote the range/2. The solid lines represent the best fits to the Michaelis–Menten equation (for N5-Pan) or to Eqn (5) (for dN5). (C) Inhibition profiles for *Sa*PanK$_{II}$ as described for *Ec*PanK$_I$ in (A). (D) Kinetic profiles for *Sa*PanK$_{II}$ with Pan in the presence of increasing concentrations of dN5 (indicated on the right of each curve). The data points represent the mean of two independent experiments, each performed in triplicate; the error bars denote the range/2. The solid lines represent the best fit curves obtained by fitting Eqn (2) to all the data; the shaded areas indicate the 90% confidence intervals. The insert shows the stimulatory effect of the inhibitor at low substrate concentrations which results from the change Pan's saturation kinetics profile from sigmoidal for Pan only (black) to hyperbolic for Pan in the presence of 3.75 μM dN5 (purple).

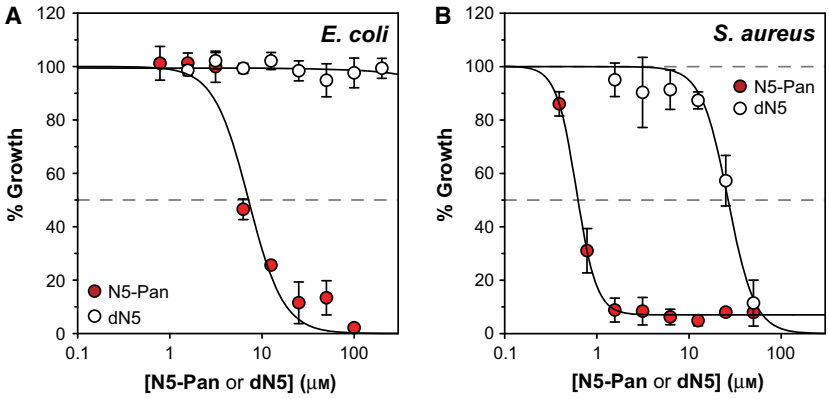


**Fig. 6.** dN5 as a bacterial cell growth inhibitor. (A) Growth inhibition profiles for *E. coli* grown in minimal medium in the presence of increasing concentrations of N5-Pan and DL-4′-deoxy-N5-Pan (dN5). The data points represent the mean of two independent experiments, each performed in triplicate; the error bars denote the range/2. The solid lines represent the best fits to Eqn (5). (B) Growth inhibition profiles for *S. aureus* grown in minimal medium as described for *E. coli* in (A).

inhibition of *S. aureus* growth mimic the interactions of PantSH with *Sa*PanK$_{II}$.

## Discussion

Although several previous studies have investigated the growth inhibitory potency of pantothenamides against various bacteria, and/or have shown that these compounds act as substrates of the target organisms' PanK enzymes, none have been able to establish a clear link between these two features [1,6–8,12,14–16,26,32,37]. In the present study, we performed the first detailed comparative kinetic analysis of pantothenamides that cause bacterial growth inhibition, showing that PanK type determines their mode of action. For organisms with PanK$_I$ enzymes, our data indicate that pantothenamides only show growth inhibition if they are accepted as alternate PanK substrates. This corresponds to these compounds having a mode of action

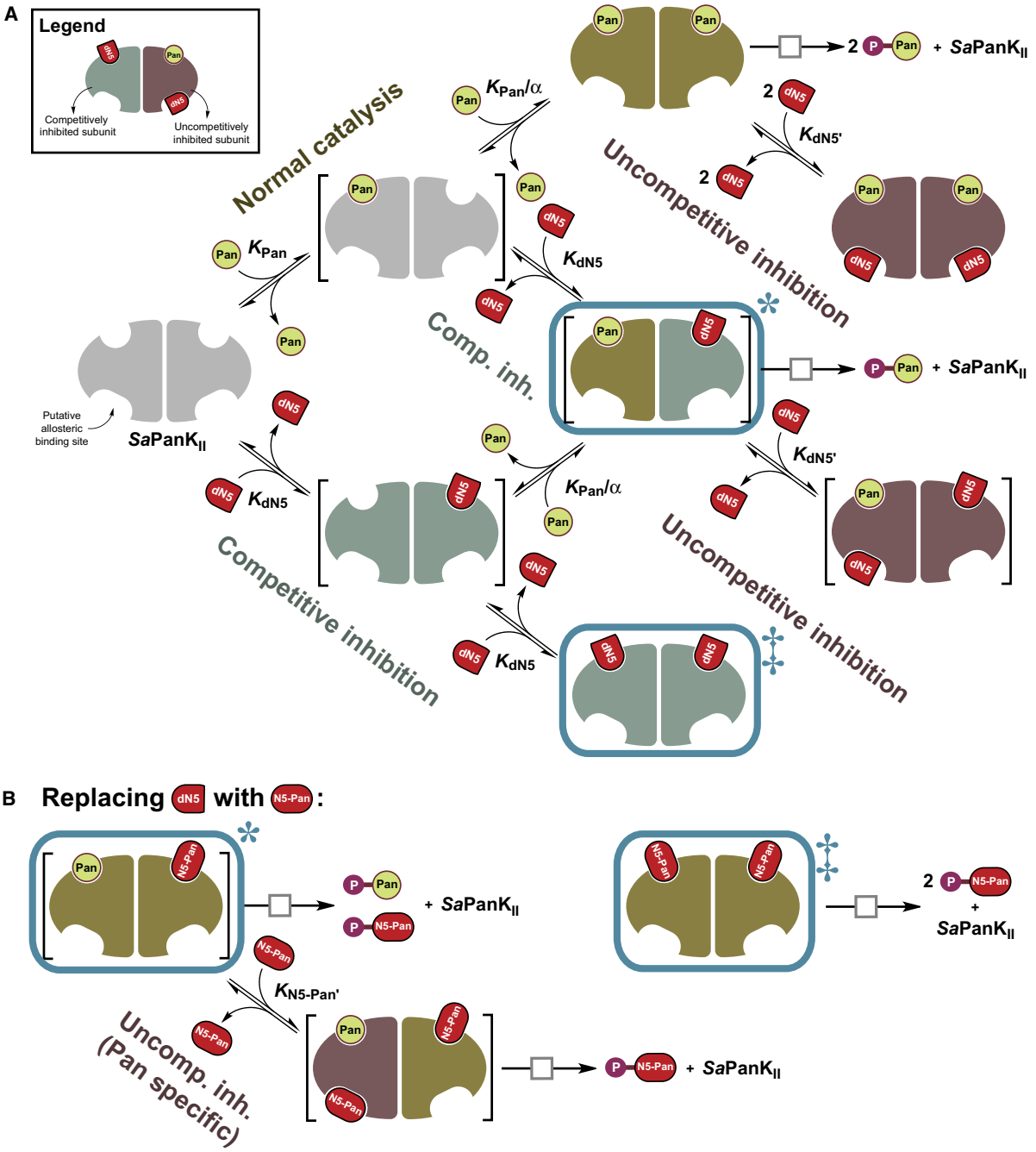


**Fig. 7.** Kinetic model for the interaction of dN5 and N5-Pan with *Sa*PanK$_{II}$. (A) Schematic representation of the *Sa*PanK$_{II}$ kinetic model adapted to account for the dual stimulatory/inhibitory effect shown by d5N. $K_{Pan}$ is the dissociation constant of Pan and α denotes the change in dissociation constant in the enzyme form with Pan bound to both subunits. $K_{dN5}$ denotes the dissociation constant for competitive inhibition, whereas $K_{dN5'}$ is the dissociation constant for uncompetitive inhibition. Note that, for the latter, it is assumed that inhibition takes place through binding at an allosteric site as shown, although no evidence for such a site has yet been found. For enzyme complexes shown in square brackets, the symmetrical alternative complex is not shown but implied. All active enzyme subunits are shown in green, whereas the competitively and uncompetitively inhibited complexes are shown in shades of grey as indicated. (B) The model shown in (A) can be modified to account for the interaction of the N5-Pan with *Sa*PanK$_{II}$ by converting the two competitively inhibited complexes [boxed and identified with an asterisk (*) and double dagger (‡), respectively] to catalytically active complexes that phosphorylates N5-Pan (and Pan) as indicated. $K_{N5\text{-}Pan'}$ is the dissociation constant for the uncompetitive inhibition shown by N5-Pan.

**Table 3.** Kinetic parameters for *Sa*PanK$_{II}$ determined from fitting various data sets to the indicated equations.

| Data set | Equation | Parameter | Value[a] | Unit |
|---|---|---|---|---|
| dN5 inhibition data (Fig. 5D) | Eqn (2) | $V_{max}$ | 6.47 ± 0.15 | μmol·min$^{-1}$·mg |
| | | $K_{Pan}$ | 9.31 ± 0.70 | μM |
| | | α | 0.111 ± 0.017 | |
| | | $K_{dN5}$ (competitive inhibition) | 3.81 ± 0.45 | μM |
| | | $K_{dN5'}$ (uncompetitive inhibition) | 41.0 ± 7.1 | μM |
| Pan:N5-Pan mix data (Fig. 4B; Fig. 8A) | Eqn (3) | $V_{max}^{N5\text{-}Pan}$ | 0.755 ± 0.100 | μmol·min$^{-1}$·mg |
| | | $K_{N5\text{-}Pan}$ (substrate) | 2.22 ± 0.48 | μM |
| | | $K_{N5\text{-}Pan'}$ (uncompetitive inhibition) | 4.89 ± 0.66 | μM |
| Pan:PantSH mix data (Fig. 8C) | Eqn (3)[b] | $V_{max}^{PantSH}$ | 0.656 ± 0.061 | μmol·min$^{-1}$·mg |
| | | $K_{PantSH}$ (substrate) | 0.46 ± 0.08 | μM |
| | | $K_{PantSH'}$ (uncompetitive inhibition) | 6.03 ± 1.27 | μM |

[a]Errors indicate the SE.
[b]PantSH replaces N5-Pan in Eqn (3) as written.

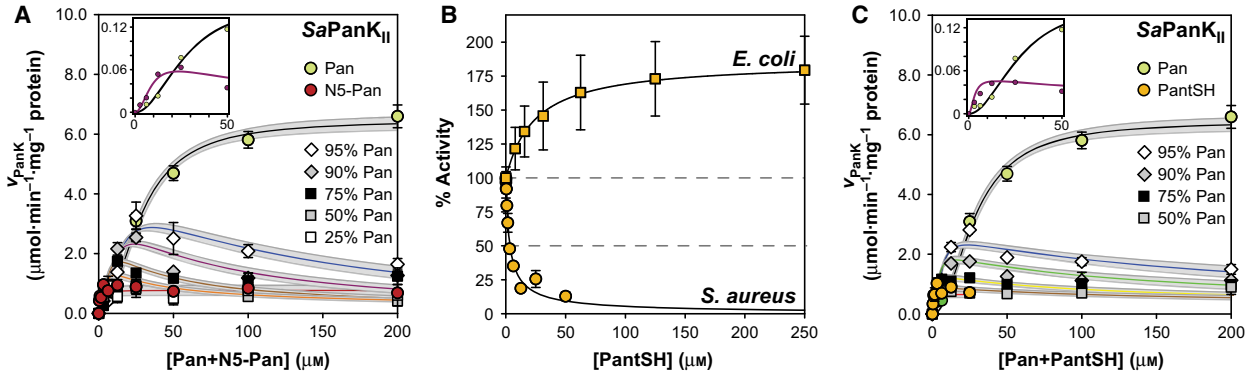


**Fig. 8.** The interaction of *Sa*PanK$_{II}$ with PantSH mimics that of N5-Pan. (A) Fitting Eqn (3) to the data obtained from *Sa*PanK$_{II}$ acting on mixtures of Pan and N5-Pan (Fig. 3B); the solid lines represent the best fit curves, whereas the shaded areas indicate the 90% confidence intervals. The insert shows the stimulatory effect caused by the presence of 5% N5-Pan (purple) compared to the 100% Pan curve (black). (B) Inhibition profiles for *Ec*PanK$_I$ and *Sa*PanK$_{II}$ treated with PantSH at a fixed concentration of 25 μM Pan. The data points represent the mean of two independent experiments, each performed in triplicate; the error bars denote the range/2. The solid lines represent the best fits to the Michaelis–Menten equation (for *Ec*PanK$_I$) or Eqn (S5) (for *Sa*PanK$_{II}$). (C) Kinetic profiles of mixtures of Pan and PantSH determined with *Sa*PanK$_{II}$ performed and analyzed as for (A).

that is dependent on their metabolic activation to form inhibitory CoA antimetabolites and/or inactive *crypto*-ACPs, and that these act as inhibitors of target(s) downstream of CoA biosynthesis. Such an analysis is in agreement with the conclusions of previous studies [8,12] and is supported by recent crystallographic data showing that growth inhibitory pantothenamides bind to PanK$_I$ enzymes in a manner similar to Pan [38,39].

For *S. aureus*, which is the only bacterium known to have an active type II PanK, the situation is very different. Specifically, we demonstrate that growth inhibitory pantothenamides have a complex interaction with this organism's PanK enzyme, acting as substrates that stimulate its activity when present at low concentrations but turning into uncompetitive inhibitors as their concentrations gradually increase. Additionally, we show that a pantothenamide analogue that cannot act as PanK substrates can still inhibit *S. aureus* growth. Taken together, these results clearly show that, in this organism, growth inhibition is likely the result of several factors working in combination: first, by being converted into CoA antimetabolites and *crypto*-ACPs (and having concomitant negative effects on fatty acid biosynthesis as was found in a previous study) [14] and, second, by reducing CoA levels by inhibiting the first step of its biosynthesis. This multifaceted mode of action is most likely one of the reasons why the pantothenamides (such as N7-Pan) show much higher potency against

*S. aureus* than any other bacterium that has been tested to date.

The kinetic model that was constructed for *Sa*PanK$_{II}$ provides an accurate description of the various data sets obtained for the enzyme acting on its native substrate (Pan), on various pantothenamides and on combinations of the two. Specifically, our model indicates that *Sa*PanK$_{II}$ is inhibited by the pantothenamides (and by PantSH) via an uncompetitive mechanism, which would imply the existence of an allosteric site in which *n*-PanAm series compounds bind. However, only two *Sa*PanK$_{II}$ structures have been deposited in the Protein Data Bank to date, neither of which has the natural substrate Pan bound. These structures provide no indication of the likely location of such an allosteric site. Moreover, the more recently published structure [i.e. that of a ternary complex of the enzyme bound to a phosphorylated pantothenamide (N354-Pan) and ADP (Protein Data Bank code: 4NB4)] [39] indicates that the enzyme has distinct open and closed conformations, with the latter preventing the product from being released; this discovery complicates the structural investigation of a potential uncompetitive inhibition mode through allosteric inhibition even further. Consequently, we cannot exclude the possibility that alternative kinetic models (including those that do not need to invoke the existence of an allosteric site) could also provide accurate descriptions of our data. Nonetheless, our proposed mechanism is the simplest one giving an accurate description of the total data set at the same time as taking all the information that is currently available on the enzyme into account.

Regardless of the mechanism or structural basis of the interaction between the growth inhibitory pantothenamides and *Sa*PanK$_{II}$, our finding that PantSH (the only pantothenamide known to occur naturally) [40,41] mirrors this complex and specific interaction suggests that it is a native ligand of the enzyme. Such a characteristic could be a compensatory regulatory mechanism for *Sa*PanK$_{II}$ because, unlike other type I and type II PanKs, this enzyme does not experience any feedback inhibition by CoA or its thioesters [14]. This is most likely as result of *S. aureus* maintaining higher levels of intracellular CoA as part of its unique redox biology because it does not contain any glutathione but instead uses CoA (and most likely the recently discovered low molecular weight thiol bacillithiol), as well as a highly specific CoA disulfide reductase, to maintain its intracellular redox potential [42,43]. Our findings suggest that CoA biosynthesis in *S. aureus* may be regulated by a unique mechanism in which PantSH stimulates *Sa*PanK$_{II}$ activity when it is present at low concentrations but inhibits it at high concentrations. Such an analysis is supported by previous findings showing that P-PantSH does not accumulate in either intra- or extracellular compartments, confirming that the regulation of CoA biosynthesis in *S. aureus* apparently occurs at the level of *Sa*PanK$_{II}$ [14].

Clearly, such a conclusion has important implications for *S. aureus* physiology that will have to be explored further, especially in light of the fact that the CoA and ACP degradation pathways responsible for PantSH formation remain very poorly characterized in all organisms [2]. Nonetheless, the evidence reported in the present study suggests that the specific interaction of *Sa*PanK$_{II}$ with PantSH presents a unique opportunity for the development of new antistaphylococcal agents, one which the pantothenamides have already started to exploit.

## Materials and methods

### General materials and methods

All the pantothenamides and precursors were prepared and their purity confirmed by $^{1}$H NMR analysis, as described previously [23]. The pantothenamides were dissolved in 50% acetonitrile–water solution to yield stock solutions at a concentration of 50 mM and assays were performed with the final acetonitrile concentration never exceeding 3% (v/v). Pantetheine was obtained by the reduction of the disulfide pantethine (Sigma-Aldrich, St Louis, MO, USA) in the presence of 1.5 equivalents of dithiothreitol or tris(2-carboxyethyl)phosphine. General chemicals, reagents and media were purchased from Sigma-Aldrich, Merck Chemicals (Darmstadt, Germany) or Acros Organics (Thermofisher, Fair Lawn, NJ, USA) and were of the highest purity. Solvents used for reactions were Chromasolv HPLC grade solvents (Sigma-Aldrich) and the hexanes, dichloromethane and ethyl acetate used for purification were purchased from Merck Chemicals. Dry *N*,*N*-dimethylformamide was prepared by shaking up over potassium hydroxide, distilled under reduced pressure and a nitrogen atmosphere, and finally stored over 4-Å molecular sieves in the dark. Dry dichloromethane was distilled from $CaH_2$ under a nitrogen atmosphere.

The *E. coli* K12 strain was available in our laboratory, whereas *S. aureus* RN4220 and *P. aeruginosa* ATCC 27853 where kind gifts from L. M. T. Dicks at the Department of Microbiology (Stellenbosch University). *Ec*PanK$_{I}$ and *Sa*PanK$_{II}$ were overexpressed and purified as described previously [7,14,34]. PK and LDH used in the kinetic assays were obtained from Roche (Basel, Switzerland).

All $^{1}$H and $^{13}$C NMR spectra were obtained using a 300-MHz Varian VNMRS (75 MHz for $^{13}$C) or 400-MHz Varian Unity Inova (100 MHz for $^{13}$C) instruments (Varian

Inc., Palo Alto, CA, USA) at the Central Analytical Facility (CAF) of the University of Stellenbosch. All chemical shifts (δ) were recorded using the residual solvent peak and reported in p.p.m. All high resolution mass spectrometry (HRMS) was performed on a Waters API Q-TOF Ultima spectrometer (Waters, Milford, MA, USA) at the MS unit of CAF. All $OD_{600}$ measurements and kinetic studies were performed using a Thermo Varioskan spectrophotometer (Thermo Scientific, Bremen, Germany). Inhibition studies were performed in Greiner Bio-One Cellstar flat-bottomed 96-well suspension plates (Greiner Bio-One GmbH, Frickenhausen, Germany). Kinetic studies were performed in Greiner Bio-One polystyrene flat-bottomed 96-well plates. The MICs were determined by plotting the percentage (relative to a control containing no inhibitor) bacterial cell growth against the logarithm of increasing compound concentration, followed by fitting Eqn (5) to the data (with the values of $y_0$ and $a$ generally fixed at 0 and 100, respectively).

$$y = y_0 + \frac{a}{1 + \left(\frac{x}{IC_{50}}\right)^b} \quad (5)$$

Kinetic data were fitted according to the derived equations. Analysis of all concentration–response curves and kinetic data was carried out using SIGMAPLOT, version 12 (Systat Software Inc., Chicago, IL, USA) or MATHEMATICA (Wolfram Research, Champaign, IL, USA).

## Synthesis of dN5

### Benzyl-3-oxo-3(pentylamino)propylcarbamate

Pentylamine (803 μL, 6.96 mmol) and diethyl phosphoryl cyanide (1.05 mL, 7.25 mmol) were added to a solution of CBz-β-alanine (1.41 g, 6.32 mmol) in dry *N*,*N*dimethylformamide (8 mL) at room temperature. The reaction mixture was cooled to 0 °C before triethylamine (1.85 mL, 13.3 mmol) was added. The reaction mixture was stirred for 2 h at 0 °C and left to stir overnight at room temperature. Ethyl acetate (50 mL) was added and the organic layer was washed sequentially with 5% citric acid (3 × 10 mL), 1 M aqueous $NaHCO_3$ (2 × 10 mL) and saturated sodium chloride (1 × 10 mL). The organic layer was dried ($Na_2SO_4$), filtered and concentrated *in vacuo* before purification by flash column chromatography (3:2 to 4:1 ethyl acetate:hexanes) afforded the carbamate (1.50 g, 81%) as a white solid. $R_f$ = 0.18. $\delta_H$ (300 MHz; $CDCl_3$) 0.87 (3H, t, $J$ = 6.9 Hz, $-CH_3$), 1.26–1.33 (4H, m, $-CH_2-$), 1.54 (2H, m, $-CH_2-$), 2.38 (2H, t, $J$ = 6.0 Hz, $-CH_2-$), 3.19 (2H, q, $J$ = 7.2, 12.9 Hz, $-CH_2-$), 3.45 (2H, q, $J$ = 6.2, 11.8 Hz, $-CH_2-$), 5.09 (2H, s, $-CH_2-$), 5.34 (2H, br s, –NH–) and 7.32–7.36 (5H, m, –CH–). $\delta_C$ (400 MHz; $CDCl_3$; 25 °C) 14.0, 22.3, 29.0, 29.2, 36.1, 37.1, 39.5, 66.6, 128.0, 128.1, 128.5, 136.5, 156.8 and 171.3. HRMS: $m/z$ $[M+H]^+$ 293.1866 (calculated $[C_{16}H_{25}N_2O_3]^+$ = 293.1860).

### 3-Amino-*N*-pentylpropanamide

Benzyl-3-oxo-3(pentylamino)propylcarbamate (1.50 g, 5.13 mmol) was dissolved in methanol (80 mL) at room temperature followed by the addition of palladium on activated carbon (Pd/C) (80.0 mg, 0.752 mmol). The reaction mixture was stirred overnight at room temperature under a $H_2$ gas balloon. Additional Pd/C (100 mg, 0.940 mmol) was added and the reaction mixture was stirred for a further 5 h under $H_2$. The reaction mixture was filtered and concentrated *in vacuo* to give the desired amide (800 mg, 99%) as a white solid. $R_f$ = 0.05 (10% methanol/dichloromethane). $\delta_H$ (300 MHz; $CDCl_3$) 0.87 (3H, t, $J$ = 7.1 Hz, $-CH_3$), 1.29–1.33 (4H, m, $-CH_2-$), 1.50 (2H, m, $-CH_2-$), 2.28 (2H, t, $J$ = 5.6 Hz, $-CH_2-$), 2.98 (2H, t, $J$ = 6.1 Hz, $-CH_2-$), 3.20 (2H, q, $J$ = 7.3, 12.9 Hz, $-CH_2-$) and 6.85 (1H, br s, –NH–). $\delta_C$ (300 MHz; $CDCl_3$; 25 °C) 14.4, 22.7, 29.5, 29.6, 38.0 38.3, 39.7 and 172.4. HRMS: $m/z$ $[M+H]^+$ 159.1499 (calculated $[C_8H_{19}N_2O]^+$ = 159.1492).

### 3,3-Dimethyl-2-oxo-butyric acid

A solution of pinacolone (10 mL, 83.4 mmol) in water (160 mL) was added to a solution of NaOH (8.00 g, 200 mmol) and potassium permanganate (12.2 g, 77.2 mmol) in water (196 mL) at 0 °C. The reaction mixture was stirred for 1 h at 0 °C, allowed to warm up to room temperature and stirred for an additional 2 h. The reaction mixture was filtered through celite, acidified to pH 2 with concentrated sulphuric acid, and the aqueous layer was extracted with diethyl ether (3 × 40 mL). The combined organic extracts were dried ($Na_2SO_4$), filtered and concentrated *in vacuo*. Bulb-to-bulb distillation (110 °C, 27.5 mmHg) gave the acid (3.99 g, 77%) as a clear oil. $\delta_H$ (300 MHz; $CDCl_3$) 1.23–1.33 (9H, m, $-CH_3$). $^1H$ NMR data are consistent with those reported previously [44].

### 3,3-Dimethyl-2-oxo-*N*-[3-oxo-3-(pentylamino)propyl] butanamide

*N*,*N*-Diisopropylethylamine (1.23 mL, 7.06 mmol) was added dropwise over 5 min to a solution of 3-amino-*N*-pentylpropanamide (800 mg, 5.06 mmol) in dichloromethane (40 mL) at 0 °C. Hydroxybenzotriazole (172.2 mg, 1.27 mmol), 3,3-dimethyl-2-oxo-butyric acid (820 mg, 6.30 mmol) and 1-ethyl-3-(3-dimethylaminopropyl) carbodiimide hydrochloride (1.34 g, 6.99 mmol) were then added consecutively and the reaction mixture was stirred overnight at room temperature. The reaction was quenched by the addition of 3 M HCl (50 mL) and the organic layer was washed with 3 M HCl (1 × 50 mL) and saturated $NaHCO_3$

(1 × 50 mL). The organic layer was dried ($Na_2SO_4$), filtered and concentrated *in vacuo* before purification by flash column chromatography (0.75 : 1 ethyl acetate : hexanes) afforded the desired amide (700 mg, 57%) as a white solid. $R_f$ = 0.27. $\delta_H$ (300 MHz; $CDCl_3$) 0.75 (3H, t, $J$ = 7.0 Hz, –$CH_3$), 1.14–1.19 (13H, m, –$CH_3$–, –$CH_2$–), 1.33–1.40 (2H, m, –$CH_2$–), 2.34 (2H, t, $J$ = 6.1 Hz, –$CH_2$–), 3.07 (2H, q, $J$ = 7.0, 13.1 Hz, –$CH_2$–), 3.42 (2H, q, $J$ = 6.1, 12.6 Hz, –$CH_2$–), 5.57 (1H, br s, –NH–) and 7.47 (1H, br s, –NH–). $\delta_C$ (400 MHz; $CDCl_3$; 25 °C) 13.9, 22.3, 26.2, 29.0, 29.2, 35.2, 35.4, 39.6, 42.9, 160.4 and 170.6, 203.0. HRMS: $m/z$ $[M+H]^+$ 271.2014 (calculated $[C_{14}H_{27}N_2O_3]^+$ = 271.2016).

### DL-4′-Deoxy-*N*-pentylpantothenamide

3,3-Dimethyl-2-oxo-*N*-[3-oxo-3-(pentylamino)propyl]butanamide (700 mg, 2.89 mmol) was dissolved in methanol (28 mL) at 0 °C under an inert atmosphere followed by the addition of sodium borohydride ($NaBH_4$, 163.44 mg, 4.32 mmol) in portions. The reaction mixture was stirred for 1 h at 0 °C and left to stir overnight at room temperature. Additional $NaBH_4$ (163.44 mg, 4.32 mmol) was added and the reaction mixture was stirred for another 3 h at room temperature. The reaction was quenched by the addition of saturated ammonium chloride (28 mL) and methanol was removed *in vacuo*. The aqueous solution was extracted with ethyl acetate (3 × 30 mL) and the combined organic extracts were dried ($Na_2SO_4$), filtered and concentrated *in vacuo* to yield dN5 (760 mg, 96%) as a colourless oil. $R_f$ = 0.39 (10% methanol/dichloromethane). $\delta_H$ (300 MHz; $CDCl_3$): 0.83 (3H, t, $J$ = 7.1 Hz, –$CH_3$), 0.93–0.95 (9H, m, –$CH_3$–), 1.24–1.27 (4H, m, –$CH_2$–), 1.43–1.48 (2H, m, –$CH_2$–), 2.37 (2H, t, $J$ = 6.2 Hz, –$CH_2$–), 3.13 (2H, q, $J$ = 7.0, 13.6 Hz, –$CH_2$–), 3.47 (2H, q, $J$ = 6.6, 12.7 Hz, –$CH_2$–), 3.66 (1H, s, –CH–), 6.38 (1H, br s, –NH–) and 7.17 (1H, br s, –NH–); $\delta_C$ (400 MHz; $CDCl_3$; 25 °C): 13.9, 22.3, 25.9, 29.0, 29.2, 35.0, 35.2, 35.6, 39.6, 79.4, 171.1 and 172.7. HRMS: $m/z$ $[M+H]^+$ 273.2172 (calculated $[C_{14}H_{29}N_2O_3]^+$ = 273.2173).

## Bacterial growth inhibition tests of pantothenamide library

The MICs of the library of *N*-substituted pantothenamides (Table 1, entries 1–47) against *E. coli* K12, *S. aureus* RN4220 or *P. aeruginosa* ATCC 27853 were determined by microbroth dilution in 96-well microtiter flat-bottomed plates and turbidometric analysis at $OD_{600}$. Starter cultures of either *E. coli* K12, *S. aureus* RN4220 or *P. aeruginosa* ATCC 27853 in 1% tryptone were prepared by inoculation with four separate colonies grown on LB agar plates. The starter culture was grown to exponential phase and then diluted 10 000-fold in the same medium. A 10-μL aliquot of the diluted cell suspension was used to inoculate each well of a 96-well plate containing 100 μL of 1% tryptone broth supplemented with the specific compound of interest (diluted from 50 mM stock solutions prepared in 50% aqueous acetonitrile to aid solubility). The compounds that exhibited positive results in initial screens at 200 μM were subsequently tested at 50 μM; those that still showed inhibition at this concentration were submitted to concentration–response analysis. Final concentrations of compounds were in the range 0.039–200 μM depending on the potency of the pantothenamide. The plates were incubated at 37 °C for 20 h before the cell densities were measured ($OD_{600}$). The extent of growth in each well was determined by normalizing the $OD_{600}$ values relative to those of the negative control (containing 3% acetonitrile instead of pantothenamide), which was taken as 100% bacterial cell growth. Each compound was tested in triplicate and all experiments were repeated at least once after the initial experiment.

## Bacterial growth inhibition studies of N5-Pan and dN5 in minimal media

The inhibition of *E. coli* K12 and *S. aureus* RN4220 by N5-Pan and dN5 was tested in minimal media appropriate for each bacterium. For *E. coli*, this medium consisted of 0.8 mM $MgSO_4$, 10 mM citric acid, 60 mM $K_2HPO_4$, 20 mM $NaNH_4HPO_4$ and 0.5% glucose; for *S. aureus*, it contained 40 mM KCl, 160 mM NaCl, 5.3 mM $MgSO_4$, 30 mM $(NH_4)_2SO_4$, 0.11 mM $CaCl_2$, 1.0 mM $KH_2PO_4$, 0.02 mM $FeSO_4$, 0.04 mM $MnSO_4$, 0.03 mM citric acid, 100 mM Tris, 28 mM glucose, 0.8 mM L-arginine, 1.0 mM L-proline, 1.9 mM L-glutamic acid, 1.5 mM L-valine, 1.5 mM L-threonine, 1.0 mM L-phenylalanine, 1.3 mM L-leucine, 0.78 mM L-cysteine, 0.4 μM biotin, 6.6 μM thiamine and 16 μM nicotinic acid [45]. The inhibition was determined by concentration–response analysis as described above with minor modifications. Briefly, starter cultures of *E. coli* K12 and *S. aureus* RN4220 in 1% tryptone were inoculated with four separate colonies grown on LB agar plates. The starter culture was grown to exponential phase and then diluted 10-fold into the applicable minimal media. A 10-μL aliquot of the diluted cell suspension was used to inoculate each well of a 96-well flat-bottomed plate containing 100 μL of minimal medium. Subsequently, the media was supplemented with either N5-Pan or dN5. For *E. coli* and *S. aureus*, the final concentrations of N5-Pan varied in the range 0.781–100 μM and 0.391–50 μM, respectively; for both organisms, dN5 was varied in the range 1.56–200 μM. The plates were incubated at 37 °C for 24 h before the cell densities were measured ($OD_{600}$) and analyzed further as described above. Each compound was tested in either two (*E. coli*) or three (*S. aureus*) independent experiments, each performed triplicate.

## PanK assays

PanK activity was determined using a continuous spectrophotometric assay that coupled the production of ADP to the consumption of NADH and was monitored by the

decrease in $A_{340}$, as described previously [7]. An extinction coefficient of 6220 $M^{-1} \cdot cm^{-1}$ was used for NADH. Each 300-μL reaction mixture contained 50 mM Tris-HCl (pH 7.6), 10 mM $MgCl_2$, 20 mM KCl, 1.5 mM ATP, 0.5 mM NADH, 0.5 mM phosphoenolpyruvate, 3 units of PK, 3 units of LDH and either 3.0 μg of *Ec*PanK$_I$ or 1.5 μg of *Sa*PanK$_{II}$. When PantSH was tested as substrate, 0.5 mM of tris(2-carboxyethyl)phosphine was also added to the reaction mixture. The concentration ranges (and ratios of substrate used in the mixture experiments) are indicated as appropriate. The reaction was initiated by the addition of substrate (or mixtures of substrates, or mixtures of substrates and inhibitors) and was monitored for 5 min at 25 °C.

### Statistical analysis

Using the raw kinetic data, initial velocities were calculated for each substrate concentration (or substrate mixture, or substrate/inhibitor mixture) by linear regression of the readings made in the 50s period after the initial 10 s (i.e. the period from 10 to 60 s after the reaction was started). For each experiment, the three readings made for each data point were averaged and plotted with the SD to give the respective kinetic profile. Kinetic parameters reported in Table 2 were determined for each experiment by fitting the appropriate equation to the data; the reported values are the mean values of the parameters determined from all the individual independent experiments, and are given with errors that indicate the range/2 or SEM as appropriate. The parameters (Table 3) were determined in a global fit by minimizing the squared difference between experimental data points and model simulation of the appropriate equation, and are given with errors that indicate the SE.

## Acknowledgements

We thank Professor Willem van Otterlo for providing advice and guidance regarding the synthesis of dN5. This project was funded by grants from the National Research Foundation (NRF) of South Africa (CPR20110726000022216) and Medical Research Council of South Africa to ES. JLS is supported by the South African Research Chairs Initiative of the Department of Science and Technology and the NRF of South Africa. MdV, LB and LK were supported by bursaries from the NRF.

## Author contributions

MdV and LB contributed equally to the syntheses, growth inhibition assays and enzyme kinetic analyses, as well as to the data analysis. LK performed enzyme kinetic assays and data analysis. JLS constructed the kinetic model and performed the associated data analysis. ES conceived the project, contributed to the data analysis and wrote the paper with contributions from all of the authors.

## References

1 Clifton G, Bryant SR & Skinner CG (1970) $N^1$-(substituted) pantothenamides, antimetabolites of pantothenic acid. *Arch Biochem Biophys* **137**, 523–528.
2 Strauss E (2010) Coenzyme A biosynthesis and enzymology. In Comprehensive Natural Products II Chemistry and Biology (Mander L & Liu H-W, eds), pp. 351–410. Elsevier, Oxford.
3 Spry C, Kirk K & Saliba KJ (2008) Coenzyme A biosynthesis: an antimicrobial drug target. *FEMS Microbiol Rev* **32**, 56–106.
4 Spry C, Macuamule C, Lin Z, Virga KG, Lee RE, Strauss E & Saliba KJ (2013) Pantothenamides are potent, on-target inhibitors of *Plasmodium falciparum* growth when serum pantetheinase is inactivated. *PLoS One* **8**, e54974.
5 de Villiers M, Macuamule C, Spry C, Hyun Y-M, Strauss E & Saliba KJ (2013) Structural modification of pantothenamides counteracts degradation by pantetheinase and improves antiplasmodial activity. *ACS Med Chem Lett* **4**, 784–789.
6 Jansen PAM, Hermkens PHH, Zeeuwen PLJM, Botman PNM, Blaauw RH, Burghout P, van Galen PM, Mouton JW, Rutjes FPJT & Schalkwijk J (2013) Combination of pantothenamides with vanin inhibitors as a novel antibiotic strategy against Gram-positive bacteria. *Antimicrob Agents Chemother* **57**, 4794–4800.
7 Strauss E & Begley TP (2002) The antibiotic activity of *N*-pentylpantothenamide results from its conversion to ethyldethia-coenzyme A, a coenzyme A antimetabolite. *J Biol Chem* **277**, 48205–48209.
8 Zhang Y-M, Frank MW, Virga KG, Lee RE, Rock CO & Jackowski S (2004) Acyl carrier protein is a cellular target for the antibacterial action of the pantothenamide class of pantothenate antimetabolites. *J Biol Chem* **279**, 50969–50975.
9 Mercer AC & Burkart MD (2007) The ubiquitous carrier protein – a window to metabolite biosynthesis. *Nat Prod Rep* **24**, 750–773.
10 Jackowski S & Rock CO (1984) Turnover of the 4′-phosphopantetheine prosthetic group of acyl carrier protein. *J Biol Chem* **259**, 1891–1895.
11 Thomas J & Cronan JE (2005) The enigmatic acyl carrier protein phosphodiesterase of *Escherichia coli*. *J Biol Chem* **280**, 34675–34683.
12 Thomas J & Cronan JE (2010) Antibacterial activity of *N*-pentylpantothenamide is due to inhibition of coenzyme A synthesis. *Antimicrob Agents Chemother* **54**, 1374–1377.

13 Choudhry AE, Mandichak TL, Broskey JP, Egolf RW, Kinsland C, Begley TP, Seefeld MA, Ku TW, Brown JR, Zalacain M *et al*. (2003) Inhibitors of pantothenate kinase: novel antibiotics for staphylococcal infections. *Antimicrob Agents Chemother* **47**, 2051–2055.
14 Leonardi R, Chohnan S, Zhang Y-M, Virga KG, Lee RE, Rock CO & Jackowski S (2005) A pantothenate kinase from *Staphylococcus aureus* refractory to feedback regulation by coenzyme A. *J Biol Chem* **280**, 3314–3322.
15 Virga KG, Zhang Y-M, Leonardi R, Ivey RA, Hevener K, Park H-W, Jackowski S, Rock CO & Lee RE (2006) Structure–activity relationships and enzyme inhibition of pantothenamide-type pantothenate kinase inhibitors. *Bioorg Med Chem* **14**, 1007–1020.
16 Mercer AC, Meier JL, Hur GH, Smith AR & Burkart MD (2008) Antibiotic evaluation and *in vivo* analysis of alkynyl coenzyme A antimetabolites in *Escherichia coli*. *Bioorg Med Chem Lett* **18**, 5991–5994.
17 Brand LA & Strauss E (2005) Characterization of a new pantothenate kinase isoform from *Helicobacter pylori*. *J Biol Chem* **280**, 20185–20188.
18 Nicely NI, Parsonage D, Paige C, Newton GL, Fahey RC, Leonardi R, Jackowski S, Mallett TC & Claiborne A (2007) Structure of the type III pantothenate kinase from *Bacillus anthracis* at 2.0 Å resolution: implications for coenzyme A-dependent redox biology. *Biochemistry* **46**, 3234–3245.
19 Yang K, Eyobo Y, Brand LA, Martynowski D, Tomchick D, Strauss E & Zhang H (2006) Crystal structure of a type III pantothenate kinase: insight into the mechanism of an essential coenzyme A biosynthetic enzyme universally distributed in bacteria. *J Bacteriol* **188**, 5532–5540.
20 Hong BS, Yun MK, Zhang Y-M, Chohnan S, Rock CO, White SW, Jackowski S, Park H-W & Leonardi R (2006) Prokaryotic type II and type III pantothenate kinases: the same monomer fold creates dimers with distinct catalytic properties. *Structure* **14**, 1251–1261.
21 Strauss E, de Villiers M & Rootman I (2010) Biocatalytic production of coenzyme A analogues. *ChemCatChem* **2**, 929–937.
22 Balibar CJ, Hollis-Symynkywicz MF & Tao J (2011) Pantethine rescues phosphopantothenoylcysteine synthetase and phosphopantothenoylcysteine decarboxylase deficiency in *Escherichia coli* but not in *Pseudomonas aeruginosa*. *J Bacteriol* **193**, 3304–3312.
23 van Wyk M & Strauss E (2008) Development of a method for the parallel synthesis and purification of *N*-substituted pantothenamides, known inhibitors of coenzyme A biosynthesis and utilization. *Org Biomol Chem* **6**, 4348–4355.
24 Zhang Y-M, Chohnan S, Virga KG, Stevens RD, Ilkayeva OR, Wenner BR, Bain JR, Newgard CB, Lee RE, Rock CO *et al*. (2007) Chemical knockout of pantothenate kinase reveals the metabolic and genetic program responsible for hepatic coenzyme A homeostasis. *Chem Biol* **14**, 291–302.
25 Siudeja K, Srinivasan B, Xu L, Rana A, de Jong J, Nollen EAA, Jackowski S, Sanford L, Hayflick S & Sibon OCM (2011) Impaired coenzyme A metabolism affects histone and tubulin acetylation in *Drosophila* and human cell models of pantothenate kinase associated neurodegeneration. *EMBO Mol Med* **3**, 755–766.
26 Ivey RA, Zhang Y-M, Virga KG, Hevener K, Lee RE, Rock CO, Jackowski S & Park H-W (2004) The structure of the pantothenate kinase.ADP.pantothenate ternary complex reveals the relationship between the binding sites for substrate, allosteric regulator, and antimetabolites. *J Biol Chem* **279**, 35622–35629.
27 van der Westhuyzen R, Hammons JC, Meier JL, Dahesh S, Moolman WJA, Pelly SC, Nizet V, Burkart MD & Strauss E (2012) The antibiotic CJ-15,801 is an antimetabolite that hijacks and then inhibits CoA biosynthesis. *Chem Biol* **19**, 559–571.
28 Wittwer CT, Beck S, Peterson M, Davidson R, Wilson DE & Hansen RG (1990) Mild pantothenate deficiency in rats elevates serum triglyceride and free fatty acid levels. *J Nutr* **120**, 719–725.
29 Wittwer CT, Schweitzer C, Pearson J, Song WO, Windham CT, Wyse BW & Hansen RG (1989) Enzymes for liberation of pantothenic acid in blood: use of plasma pantetheinase. *Am J Clin Nutr* **50**, 1072–1078.
30 Shibata K, Fukuwatari T, Ohta M, Okamoto H, Watanabe T, Fukui T, Nishimuta M, Totani M, Kimura M, Ohishi N *et al*. (2005) Values of water-soluble vitamins in blood and urine of Japanese young men and women consuming a semi-purified diet based on the Japanese dietary reference intakes. *J Nutr Sci Vitaminol* **51**, 319–328.
31 Spry C, Saliba KJ & Strauss E (2014) A miniaturized assay for measuring small molecule phosphorylation in the presence of complex matrices. *Anal Biochem* **451**, 76–78.
32 Meier JL, Mercer AC, Rivera H Jr & Burkart MD (2006) Synthesis and evaluation of bioorthogonal pantetheine analogues for in vivo protein modification. *J Am Chem Soc* **128**, 12174–12184.
33 Worthington AS & Burkart MD (2006) One-pot chemo-enzymatic synthesis of reporter-modified proteins. *Org Biomol Chem* **4**, 44–46.
34 van Wyk M & Strauss E (2007) One-pot preparation of coenzyme A analogues via an improved chemo-enzymatic synthesis of pre-CoA thioester synthons. *Chem Commun*, 398–400.
35 Yang K, Strauss E, Huerta C & Zhang H (2008) Structural basis for substrate biding and the catalytic

mechanism of type III pantothenate kinase. *Biochemistry* **47**, 1369–1380.
36 Yun M, Park C-G, Kim J-Y, Rock CO, Jackowski S & Park H-W (2000) Structural basis for the feedback regulation of *Escherichia coli* pantothenate kinase by coenzyme A. *J Biol Chem* **275**, 28093–28099.
37 Akinnusi TO, Vong K & Auclair K (2011) Geminal dialkyl derivatives of *N*-substituted pantothenamides: synthesis and antibacterial activity. *Bioorg Med Chem* **19**, 2696–2706.
38 Li B, Tempel W, Smil D, Bolshan Y, Schapira M & Park H-W (2013) Crystal structures of *Klebsiella pneumoniae* pantothenate kinase in complex with *N*-substituted pantothenamides. *Proteins* **81**, 1466–1472.
39 Hughes SJ, Antoshchenko T, Kim KP, Smil D & Park H-W (2014) Structural characterization of a new *N*-substituted pantothenamide bound to pantothenate kinases from *Klebsiella pneumoniae* and *Staphylococcus aureus*. *Proteins* **82**, 1542–1548.
40 Peters VJ, Brown GM, Williams WL & Snell EE (1953) Isolation of the *Lactobacillus bulgaricus* factor from natural sources. *J Am Chem Soc* **75**, 1688–1691.
41 Jackowski S & Rock CO (1984) Metabolism of 4′-phosphopantetheine in *Escherichia coli*. *J Bacteriol* **158**, 115–120.
42 Van Laer K, Hamilton CJ & Messens J (2013) Low-molecular-weight thiols in thiol-disulfide exchange. *Antioxid Redox Signal* **18**, 1642–1653.
43 Gaupp R, Ledala N & Somerville GA (2012) Staphylococcal response to oxidative stress. *Front Cell Info Microbiol* **2**, 33.
44 Tuck KL, Saldanha SA, Birch LM, Smith AG & Abell C (2006) The design and synthesis of inhibitors of pantothenate synthetase. *Org Biomol Chem* **4**, 3598–3610.
45 Rudin L, Sjöström J-E, Lindberg M & Philipson L (1974) Factors affecting competence for transformation in *Staphylococcus aureus*. *J Bacteriol* **118**, 155–164.